Atmósfera 39, 49-75 (2025)
https://doi.org/10.20937/ATM.53385

Satellite precipitation product assessment and correction technique selection at sub-basin scale for maximum annual events. Case study: Acaponeta River basin

Edith BONILLA-LÓPEZ[1]*, René LOBATO-SÁNCHEZ[2], Josué MEDELLÍN-AZUARA[3] and Carlos PATIÑO-GÓMEZ[1†]

[1] *Departamento de Ingeniería Civil y Ambiental, Universidad de las Américas Puebla, 72810 San Andrés Cholula, Puebla, México.*
[2] *Instituto Mexicano de Tecnología del Agua, 62550 Jiutepec, Morelos, México.*
[3] *Department of Civil and Environmental Engineering, University of California Merced, Merced, CA 95343, USA.*
*Corresponding author; email: edith.bonillalz@udlap.mx

Received: March 21, 2024; Accepted: September 17, 2024

RESUMEN

La escasez y discontinuidad de observaciones de precipitación a diferentes escalas espaciotemporales y la necesidad de realizar estudios hidrológicos detallados han incrementado el uso de datos satelitales de precipitación. Sin embargo, es necesario revisar y corregir el sesgo entre la precipitación observada y estimada. Este trabajo evalúa el producto CHIRPSv2.0 para eventos máximos anuales y diferentes condiciones climatológicas a partir de observaciones, utilizando métricas estadísticas y seleccionando el método de corrección de sesgo apropiada (a escala puntual y de subcuenca) a partir de las técnicas de escala lineal, escala de intensidad local o transformación de potencia. Con ello se optimizan los registros de precipitación anual máxima del periodo 2001-2020 para la cuenca del Río Acaponeta, México. Aplicaciones previas han analizado escalas temporales mayores. Se identificaron diferencias en el rendimiento de los métodos de corrección entre las escalas de punto y subcuenca. La transformación de potencia presentó un buen rendimiento a escala puntual, pero el sesgo porcentual a escala subcuenca resultó en una gran sobreestimación en la zona superior, para los años medio y seco, y en la parte inferior para el año húmedo. Por su parte, la escala lineal y la escala de intensidad local lograron una buena reducción del sesgo porcentual en los puntos, si bien la primera sobreestimó los datos a nivel de subcuenca para todas las regiones. La técnica de escala de intensidad lineal mostró mejores correcciones en las zonas media y baja, y mayor sobreestimación en las cuencas altas para los años medio y húmedo. Los valores máximos anuales corregidos tienen gran utilidad para el análisis hidrológico en el contexto de la evaluación del riesgo de inundaciones.

ABSTRACT

Satellite precipitation products (SPP) are increasingly being used for detailed hydrological studies due to scarce and discontinuous precipitation observations at different spatial and temporal scales. However, to evaluate its full utility, it is necessary to assess and correct the bias between estimated and observed precipitation (OP). The aim of this paper is to evaluate the CHIRPSv2.0 product for maximum annual events and different climatological conditions based on in-situ observations, using statistical metrics and selecting from linear scaling (LS), local intensity scaling (LOCI) and power transformation (PT) the appropriate bias correction technique (CT), at point and sub-basin scale, improving the maximum annual precipitation records for the period 2001-2020 in the Acaponeta River basin, Mexico. Previous applications of bias CT have focused on broader temporal scales rather than specific maximum events. Differences in the performance of the correction methods were identified between point and sub-basin scales. PT presented a good performance

© 2025 Universidad Nacional Autónoma de México, Instituto de Ciencias de la Atmósfera y Cambio Climático.
This is an open access article under the CC BY-NC License (http://creativecommons.org/licenses/by-nc/4.0/).

at the point scale, in contrast to percentual bias (PBIAS), which resulted in a great overestimation at the sub-basin scale in the upper zone for the average and dry years, while for the wet year, it overestimated in the lower part. Although LS and LOCI generally observed a good PBIAS reduction at the gauge stations, LS overestimated at the sub-basin scale overall. LOCI showed better SPP corrections in the middle and lower zones and a wider range of overestimation for the upper basins in the middle and wet years. The corrected annual maximum estimated values for the revised period are useful for hydrological analysis in the context of flood risk assessment.

Keywords: satellite rainfall estimates, CHIRPS, bias adjustment, annual maximum events, local intensity scaling, Acaponeta River basin (Mexico).

1. Introduction

Since precipitation is one of the main triggers of runoff, its measurement and monitoring are of great importance. Nevertheless, observed precipitation (OP) data in some regions is scarce and discontinuous. The lack of accurate and sufficient precipitation data at specific temporary and spatial scales and the increasing development of global databases for different climatic and environmental variables, like satellite precipitation products (SPP), merit assessing the biases between SPP and the limited observations. Such assessments allow for characterizing the feasibility of using SPP in scientific studies, particularly to analyze extreme precipitation related to flood events. Reviewing the need for rainfall data associated with annual maximum events is relevant not only for analyzing the behavior of this climatological variable in time but also because of its practical use in flood protection and management, runoff storage, and storm drainage infrastructure, as well as being the technical basis for decision making for protecting the population against flood disasters.

The evaluation of several SPP for different purposes has been developed in literature, mainly regarding the Tropical Rainfall Measuring Mission (TRMM) (Derin and Yilmaz, 2014; de Jesús et al., 2016; Ávila-Carrasco et al., 2018; Soo et al., 2020; Morales-Velázquez et al., 2021), the Integrated Multisatellite Retrievals for the Global Precipitation Measurement (IMERG) (Mayor et al., 2017; Soo et al., 2020; Aksu et al., 2023), the Climate Prediction Center Morphing Technique (CMORPH) (Derin and Yilmaz, 2014; Bhatti et al., 2016; Soo et al., 2020) and its corrected bias version (CMORPH-CRT) (Bruster-Flores et al., 2019), the Climate Hazards Group Infrared Precipitation with Station (CHIRPS) (Perdigón-Morales et al., 2018; Morales-Velázquez et al., 2021; Aksu et al., 2022; González-Ortigoza et al., 2023; Villate et al., 2023), the Global Satellite Mapping of Precipitation (GSMaP) (Saber and Yilmaz, 2018; Yeh et al., 2020), and the Precipitation Estimation from Remotely Sensed Information using Artificial Neural Networks (PERSIANN) (Soo et al., 2020; Ceferino-Hernández et al., 2024), among other datasets. From these studies, different sources of bias were identified, such as topographic configuration, orography, location, image processing, seasonality, climatology, thresholds, poor correction of estimates with observed data, and the potential bias associated with the uncertainty of observations.

An important source of SPP bias is the topographic configuration, mainly orography, as it redirects moisture-laden air masses upwards, cooling them and precipitating their moisture (NOAA, 2023). A connection between orography, extreme heavy rainfall, and tropical or subtropical systems is presented in Huang and Lin (2014). As compiled by literature, the influence of orography on the occurrence of rainfall in mountainous regions can result in the presence of different microclimatic conditions, an increase in mean annual precipitation rates within higher elevations, and the interaction of large-scale circulation effects with topography, which determined the spatial distribution (Chen et al., 2022; Srivastava et al., 2022). Adhikari and Behrangi (2022) studied the challenges of SPP in complex terrain regions to detect and estimate this climatic variable due to the type of sensors used for this purpose, from radar, passive microwave imager/sounder, or infrared radiometers.

Moreover, in some regions, monthly and annual satellite precipitation estimates have a better performance than the corresponding on a daily scale (Aksu and Akgul, 2020; Du et al., 2024), as is the case of some extreme events. Saber and Yilmaz (2018), Soo et al. (2020), Morales-Velázquez et al. (2021), Aksu et al. (2023), and Villate-García et al. (2023) assessed SPP oriented to extreme precipitation and flood analysis. On the other hand, de Jesús et al. (2016), Perdigón-Morales et al. (2018), Aksu et al. (2022), and Dawa et al. (2024) evaluated the application of some of the satellite precipitation products to analyze drought conditions.

To characterize the differences between satellite data and observations, the statistical concepts of bias, mean error, Nash-Sutcliffe efficiency coefficient, root mean square error, and correlation, are commonly employed (Fang et al., 2015; Báez-Villanueva et al., 2018; Goshime et al., 2020; Morales-Velázquez et al., 2021; Ceferino-Hernández et al., 2024). In terms of rainfall, according to the scope of studies, the bias could be acceptable in a range of 5 to 10%, which is broadly consistent with the literature (Mendoza, 2019; Roque, 2023). To reduce bias, several correction techniques (CTs) have been applied to grid rainfall estimates based on in-situ observations that consider monthly examination of point-to-grid data and look to minimize the monthly bias. Some examples of CT include linear scaling (LS), local intensity scaling (LOCI), power transformation (PT), empirical quantile mapping, and multiplicative bias correction schemes (Fang et al., 2015; Bhatti et al., 2016; Belayneh et al., 2020; Soo et al., 2020; Aksu et al., 2023; González-Ortigoza et al., 2023). The various aspects to consider if satellite precipitation (SP) data is not corrected are the potential under- or over-estimations on infrastructure design, warning systems, or the development of flood risk management actions.

In Mexico, the Hydrological Information System provides a historical daily record of climatologic stations overseen by the National Meteorological Service (SMN) of the National Water Commission (CONAGUA) from 1920 to more recent periods (CONAGUA, 2019; CICESE, 2022). However, the records are discontinuous for several stations, bringing challenges to curating datasets in hydrological projects. On the other hand, CHIRPS v2.0, a global-scale satellite dataset, is available and is corroborated through data from climatologic stations in the field, with a time scale from 1981 to date at 0.05º × 0.05º degrees of spatial resolution (Funk et al., 2015). CHIRPS v2.0 can be consulted for a certain area of interest, providing weighted values, time series, and gridded datasets.

The aim of this project is to assess the bias of CHIRPS v2.0 precipitation product for maximum annual rainfall events based on in-situ observations and to select the appropriate bias CT at a sub-basin scale for the Acaponeta River basin, which is prone to flooding as a result of extreme precipitations during the rainy season and the presence of tropical cyclones (the most recent being Hurricane Willa on October 2018, tropical storm Pamela on October 2021, and hurricane Roslyn on October 2022) (CENAPRED, 2021, 2022, 2023).

To achieve this purpose, dry, average, and wet years are selected, in-situ precipitation stations with available records of the maximum annual events are located, and daily SP grids are obtained and converted to point data. With both databases, the bias is then measured by statistical metrics; LS, LOCI, and PT, CTs are applied at point scale, and correction factors (CF) for each approach are interpolated at a sub-basin scale in order to correct the daily SPP for maximum annual events defined per sub-basin on the analyzed years. Finally, the statistical metrics between corrected SPP and OP are applied at a sub-basin scale, a spatial evaluation of corrected SPP is performed, and the CT related to values near the optimal (especially for the region of the basin with less observed data) is selected as appropriate and used to correct daily satellite precipitation of maximum annual events.

The proposed methodology provides a practical technique for the correction of estimated rainfall values, which can be used in the development of projects that contribute to risk assessment due to extreme hydrometeorological phenomena such as floods, where sufficient observed precipitation data is unavailable largely due to the lack of spatially distributed measurements.

2. Data and methods

2.1 Description of the case study

The Acaponeta River basin covers an area of 5117 km^2 that includes portions of the states of Durango, Sinaloa, and Nayarit in northwestern Mexico, and the urban and agricultural area settled near the floodplain of the river is prone to flooding events and has been damaged several times (CENAPRED, 2021). The boundaries of the basin were obtained by using a digital elevation model (DEM) of 12.5 × 12.5 m resolution (JAXA, 2010), from where the total length of the main river stem was estimated at 248 km (Fig. 1a). Tropical wet-dry and temperate with dry winter climate are preponderant in the region of interest according to the national database of Köppen climate classification modified by García at a 1:1000000 spatial scale for the Mexican territory (CONABIO, 1998). The mean normal annual precipitation for the period 1991-2020 is 923 mm and the mean annual temperature is 30 ºC (INEGI, 2007; CONAGUA, 2023). Figure 2 shows the monthly accumulated precipitation from the CHIRPSv2.0 dataset at the full basin scale. The rainy season occurs from June to October, with higher values during August. The dry season takes place from November to May, with April being the month that presents the minimum precipitation. Especially for January and September, some precipitation values are more scattered.

Due to the size of the basin, its topographic characteristics, and hydrographic configuration, as well as the different soil types and uses, a disaggregation into 14 sub-basins (Fig. 1a) is considered appropriate to capture hydrological behavior, precipitation spatial distribution, and the major runoff origination area (Kite and Kouwen, 1992; Zhang et al., 2004). Following this approach, it will be possible to guide the planning for sub-basins with a higher frequency of flooding.

Figure 1a shows a lack of rainfall measurements in the middle basin area, which is an important characteristic for hydrologic studies when examining the basin's response to the spatial distribution of precipitation. In terms of topographic configuration, the basin's highest elevation is 2920 masl, and the outlet is located at approximately 1 m. Additionally, the location of in-situ measurements with respect to the terrain elevation must be considered when assessing bias, as the topographic effect affects the accuracy of satellite databases (Derin and Yilmaz, 2014; Yeh, et al., 2020). The selected climatological stations can be located in three regions: Upper, above

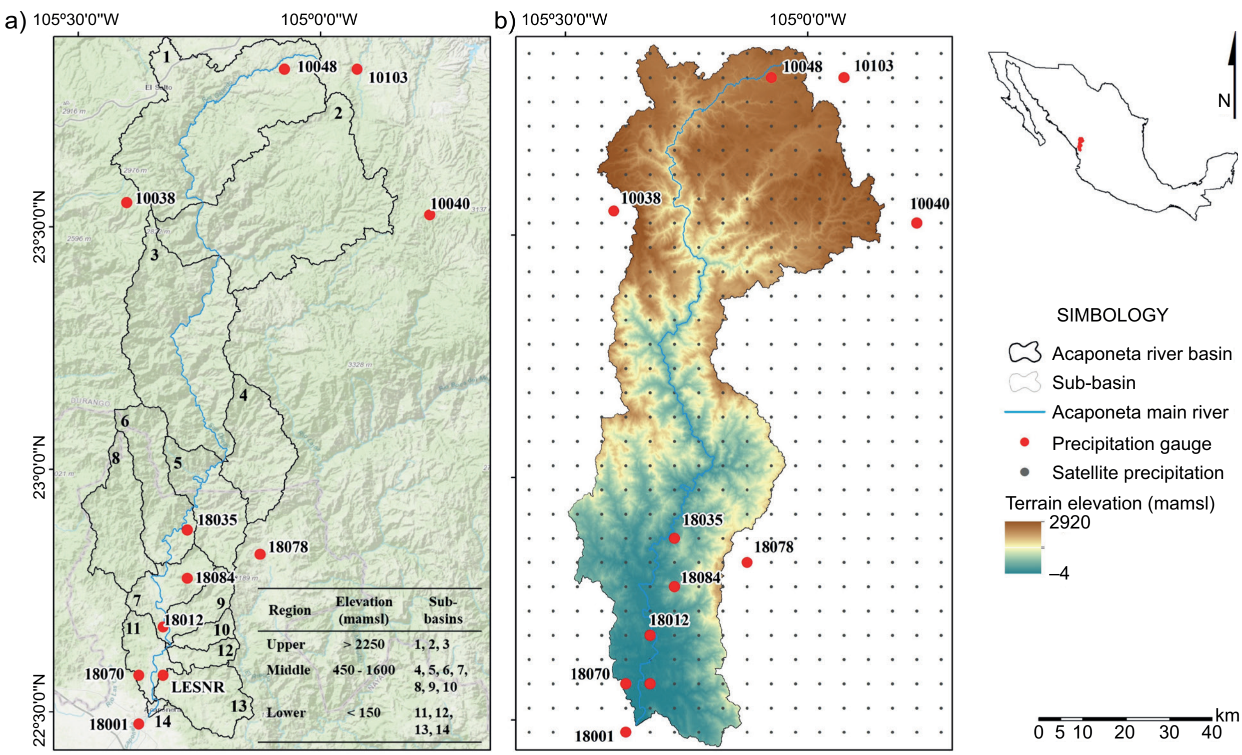

Fig. 1. (a) Configuration of the Acaponeta River basin, and (b) location of climatological stations and satellite precipitation grid points with respect to terrain elevation. (Source: self-elaboration with data from CONAGUA [2019] and JAXA [2010]).

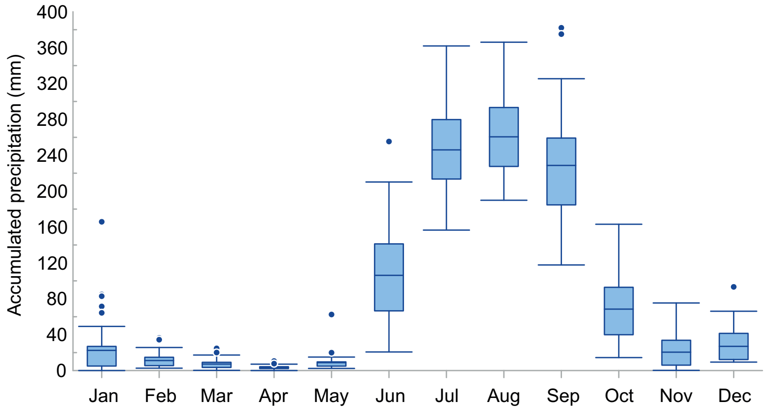

Fig. 2. Boxplot of monthly average accumulated precipitation from 1981-2020 at total basin scale. (Source: self-elaboration with the CHIRPS dataset [Funk et al., 2015]).

2250 masl, with stations 10038 (La Peña), 10040 (Las Bayas), 10048 (Navíos Viejos), and 10103 (Santa Bárbara), corresponding to the sub-basins 1 to 3; Middle, between 450 and 1600 masl, with stations 18035 (Tachichilpa), 18078 (San Andrés Milpillas) and 18084 (Mesa de Pedro y Pablo), for sub-basins 4 to 10; and sub-basins 11 to 14 as the Lower region, near the outlet of the basin, with stations 18012 (Huajicori), 18070 (La Estancia), LESNR<what is LSNR?>, and 18001 (Acaponeta), beneath 150 masl.

2.2 Data

For hydrological studies, in-situ rainfall measurements are usually scarce in space and time to represent the behavior of this variable at a basin scale. Therefore, to investigate the viability of SPP estimates to cover this information gap, the estimation of bias and selection of adequate CTs are required. To assess the performance of the bias CT, average, dry, and wet years (2007, 2009, and 2015, respectively) were selected from an analysis of the average maximum OP at the total basin scale from 1988 to 2018. Within the precipitation gauges placed on the region, the available records were revised for the temporal scenarios of interest (CONAGUA, 2019), and stations that met the record length for 2007 and 2015 and ten for 2009 were chosen (Fig. 1b).

Since fluvial floods can be generated by the occurrence of extreme precipitation events, the annual maximum events were revised for the temporal scenarios. For the Acaponeta River basin, the CHIRPS v2.0 precipitation product was employed to obtain daily gridded satellite precipitations for months corresponding to maximum annual events. This database results from combining satellite images and records of meteorological gages (Funk et al., 2015) and is available at https://climateserv.servirglobal.net/.

2.3 Methods

The workflow adopted in this research is presented in Figure 3. To establish the differences between observed and estimated rainfall data, the gridded satellite precipitation product dataset at a daily scale was converted into points at the center of each grid and compared with in-situ data records at the correspondent location. Figure 1b presents the spatial distribution of the available rainfall stations and the points with satellite information.

To assess precipitation estimates at the point to grid scale, a statistical approach was employed by estimating percentage bias (PBIAS), mean error (ME), Nash-Sutcliffe efficiency coefficient (NSE), root mean square error (RMSE), and Spearman correlation coefficient (r_s). The use of the Spearman correlation coefficient is proposed due to its robustness, low sensitivity to outliers, and nonparametric approach (Mijares-Fajardo et al., 2024), which results relevant in the case of maximum annual precipitation events in the region that do not necessarily follow a normal distribution and present outliers. Formulations of all these approaches are shown in Table I, where P_{obs} refers to the in-situ observed precipitation,

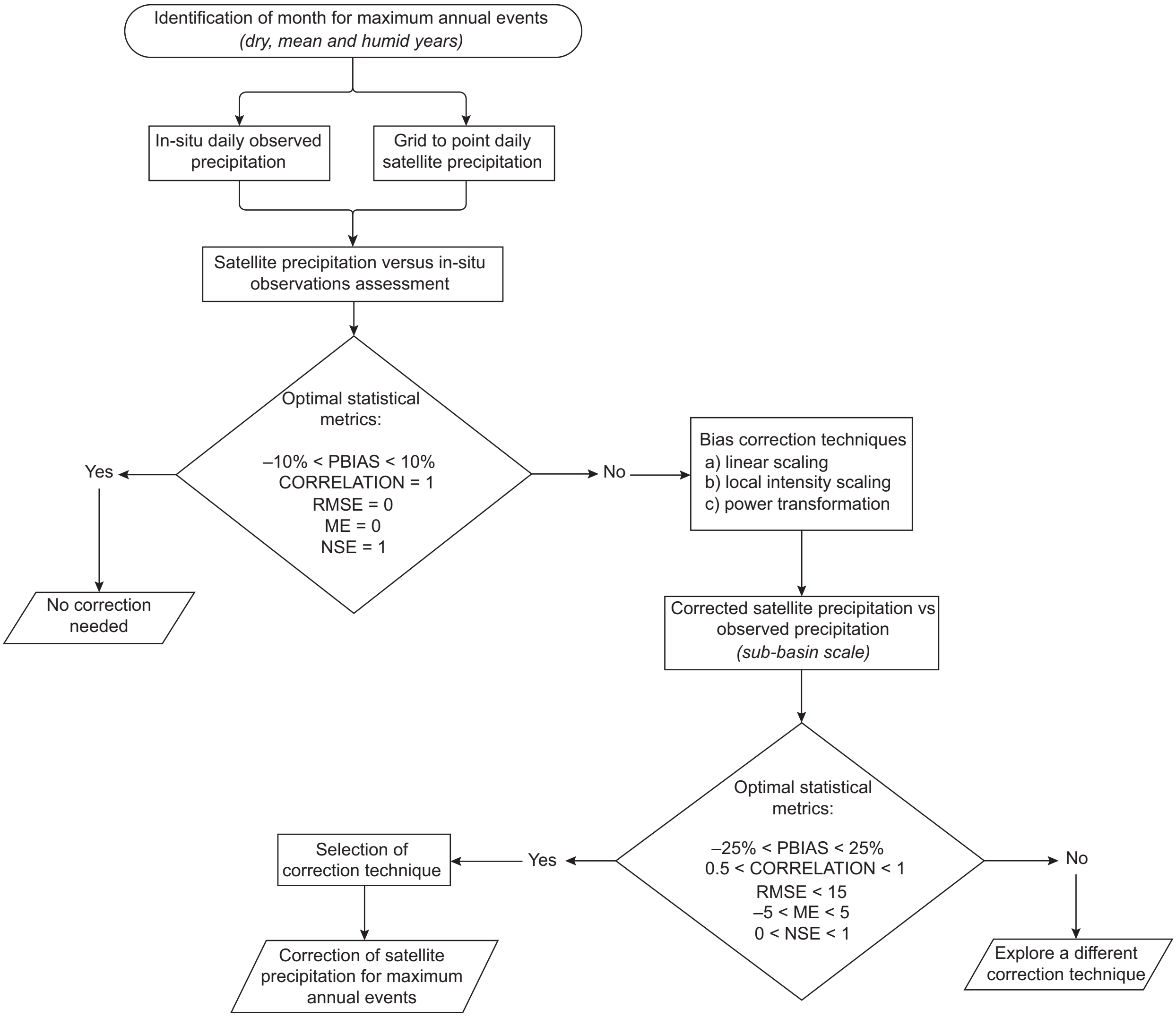

Fig. 3. Workflow for assessing and selecting correction techniques (CT) of satellite precipitation products for maximum annual events.

P_{sat} to the satellite estimates, and n is the number of observations. Toté et al. (2015), Mendoza (2019), and Roque (2023) established the ideal values of some of the mentioned numerical metrics in the case of SP analysis, hydrological purposes, and flood forecasting; ME close to 0, NSE close to 1, high values of r_s, PBIAS between 5 and 10%. Considering the interpolation process to determine the mean observed precipitation at sub-basin scale with the existing observation points, based on what has been identified in other studies (Bhatti et al., 2016; Soo et al., 2020; Nakkazi et al., 2022; Nigussie et al., 2023) around the best bias correction, the authors suggest that at sub-basin spatial scale, the optimal statistical metric values are the ones shown in Figure 3.

LS, LOCI, and PT coincide in the evaluation of the monthly mean of corrected and observed records, with the difference that LOCI considers a wet-day threshold to improve raw data (Schmidli et al., 2006), while PT searches for the correction not only for the bias but also for the variance and needs to apply previously the LOCI technique to consider wet-day probability (Teutschbein and Seibert, 2012, cited in Fang et al., 2015). The multiplicative bias correction considers different schemes of time windows, forward, central, and backward, to reduce the discrep-

Table I. Statistical metrics used for the assessments of satellite precipitation product estimates.

Statistical metric	Objective	Equation	Optimal values
Percentage bias	Illustrates the degree of correspondence of the estimated and observed mean.	$PBIAS = 100\frac{\sum(P_{sat} - P_{obs})}{\sum P_{obs}}$	5-10
Mean error	Estimate the average error of the satellite precipitation product.	$ME = \frac{1}{N}\sum(P_{sat} - P_{obs})$	0
Nash-Sutcliffe efficiency	Indicates the skill of the estimates relative to the gauge mean.	$NSE = 1 - \frac{\sum(P_{sat} - P_{obs})^2}{\sum(P_{obs} - \bar{P}_{obs})^2}$	1
Root mean square error	Reflects the error intensity and evaluates the satellite precipitation product datasets in terms of temporal dynamics.	$RMSE = \sqrt{\frac{\sum_{i=1}^{N}\left(P_{obs} - P_{sat}\right)^2}{n}}$	0
Spearman correlation coefficient	Identifies similarities or differences between variables. Used to evaluate data from independent sources in climate science. Less sensitive to outliers than Pearson's method.	$r_s = 1 - \frac{6\sum_{i=1}^{n} d_i^2}{n(n^2+1)}$	1

Source: adapted from Roque (2023), Yu et al. (2020), Ocampo-Marulanda et al. (2022), and Toté et al. (2015).

ancy between estimates and observations (Bhatti et al., 2016). For the empirical quantile mapping, the cumulative distribution function is determined for satellite precipitation products and in-situ data, and for each of the 100 quantiles, an adjustment is achieved to correct the simulated values (Lafon et al., 2013).

Nevertheless, each of the described methods behaves differently according to the conditions of the case study, and it is necessary to consider their performance in the improvement of satellite estimations for hydrological studies. In this study, LS, LOCI, and PT approaches were applied through the equations considered by each technique, as summarized in Table II. For the LS technique, $P_{cor,m,d}$ is the corrected precipitation, $P_{raw,m,d}$ corresponds to the raw value on the day *dth* of month m, and $\mu(P_{obs,m})$ refers to the mean observed precipitation value for month m. In the LOCI method, $P_{thres,m}$ is the wet day threshold for the *mth* month and *sm* is the scaling factor. Lastly, for the power transformation correction procedure, $f(bm)$ is the function to be minimized with the variable bm, $\sigma(\cdot)$ indicates the standard deviation, and $P_{LOCI,m}$ is the LOCI corrected precipitation for month m.

For each of the rain gauge points and CT, the correction factors (CFs) are identified. Since the daily satellite precipitation product is obtained at a sub-basin scale, the CFs are interpolated by Thiessen polygons and the inverse distance weighting (IDW) methodology to weight the factors for dry, average, and wet scenarios and each sub-basin. Within the available interpolation methods, as presented by Soo et al. (2020) and Bhatti et al. (2016), there are references to the good representation of the distribution of rainfall with IDW compared with Kriging or regression methods. The Thiessen method is one of the most commonly used in hydrology (Morales-Velázquez et al., 2021) and to define areal precipitation for SPP evaluation (Saber and Yilmaz, 2018; Belayneh et al., 2020; Nigussie et al., 2023), considering the spatial distribution of existing gauges. With sub-basin CF values, the daily SPP is corrected for the maximum precipitation period for the studied years.

Subsequently, to evaluate the performance, the statistical metrics of Table I are applied to the comparison between observed data and corrected SPP at the precipitation gauge points and for each of the CF interpolation approaches and CTs at the sub-basin

Table II. Bias correction techniques.

Technique	Equations	Observations
Linear scaling (LS)	$P_{cor,\,m,d} = P_{raw,\,m,d} \times \dfrac{\mu(P_{obs,m})}{\mu(P_{raw,m})}$	$P_{cor,m,d}$ is the corrected precipitation and $P_{raw,m,d}$ is the raw value, on the day *dth* of month *m*; $\mu(P_{obs,m})$ refers to the mean observed precipitation value for month *m*.
Local intensity scaling (LOCI)	$s_m = \dfrac{\mu(P_{obs,m,d} \mid P_{obs,m,d>0})}{\mu(P_{raw,m,d} \mid P_{raw,m,d} > P_{thres,m})}$ $P_{cor,m,d} = \begin{cases} 0, & if\, P_{raw,m,d} < P_{thres,m} \\ P_{raw,m,d} \times s_m & otherwise. \end{cases}$	$P_{thres,m}$ is the wet day threshold for the *mth* month and s_m is the scaling factor.
Power transformation (PT)	$f(b_m) = \dfrac{\sigma(P_{obs,m})}{\mu(P_{obs.m})} - \dfrac{\sigma(P^{b_m}_{LOCI,m})}{\mu(P^{b_m}_{LOCI,\,m})}$	$f(b_m)$ is the function to be minimized with the variable b_m, $\sigma(\cdot)$ corresponds to the standard deviation, and $P_{LOCI,m}$ is the LOCI corrected precipitation for month *m*.

Source: adapted from Fang et al. (2015).

scale. From a combination of the values of PBIAS, ME, NSE, RMSE, and r_s, a spatial representation and assessment is employed to define which of the interpolation methods and CT results in a better correction of satellite precipitation products for the studied scenarios for both point and sub-basin scale. Therefore, the approach that better characterizes the spatial precipitation distribution, especially in the middle basin area, is selected for the correction of SPP at a sub-basin scale.

3. Results

A pair-wise comparison of precipitation estimates and observed records for maximum annual events was undertaken using statistical metrics. For all climatological station's points, Figure 4 shows the statistical assessment for the studied scenarios, where a bigger range is observed for the correlation between 2007 and 2015, and low and high positive correlations were defined for most of the points in a year. In most stations in 2009, RMSE values are lower than 15 units. NSE values for all scenarios and points are far from optimal. As for 2009, lower variability within the sub-basins is recognized for all metrics. Only three and five points for 2007 and 2009, respectively, meet the acceptable values of PBIAS.

Figure 5 shows the magnitudes of the numerical metrics describing the differences between SPP estimates and in-situ observations for the maximum annual events of dry, average, and wet years over the region. Using Table I equations, PBIAS, RMSE, NSE, ME, and r_s were calculated for each point related to a climatological station and month of occurrence of the annual maximum precipitation events.

Overall, for the wet year (e.g., 2015), more PBIAS values higher than 25% are identified, and optimal quantities are observed at one point in the upper and lower basin for 2007. For 2009, the minimum PBIAS values are registered, particularly at the lower zone. Generally, at the upper basin, the mean PBIAS is approximately –15% in the three scenarios, corresponding to an overestimation of precipitation. In the middle, a mean PBIAS of 30% was estimated. Lastly, a 21% sub-estimation between SPP and OP is estimated for the lower basin points.

The lowest values of RMSE and ME occurred in the dry and average years. RMSE has the highest value in the lower basin points in the wet and average scenarios, and ME indicates generally greater differences in the lower points. Among all analyzed scenarios, the one for 2009 presents a better correlation (r_s), followed by 2015 and 2007, although the mean magnitudes correspond to low positive correlations. Regarding NSE, the lowest values were observed in 2015. Nevertheless, the higher records for 2009 are not near the optimal.

At the grid-to-point scale, the LS, LOCI, and PT correction results are shown in Figures 6, 7, and 8.

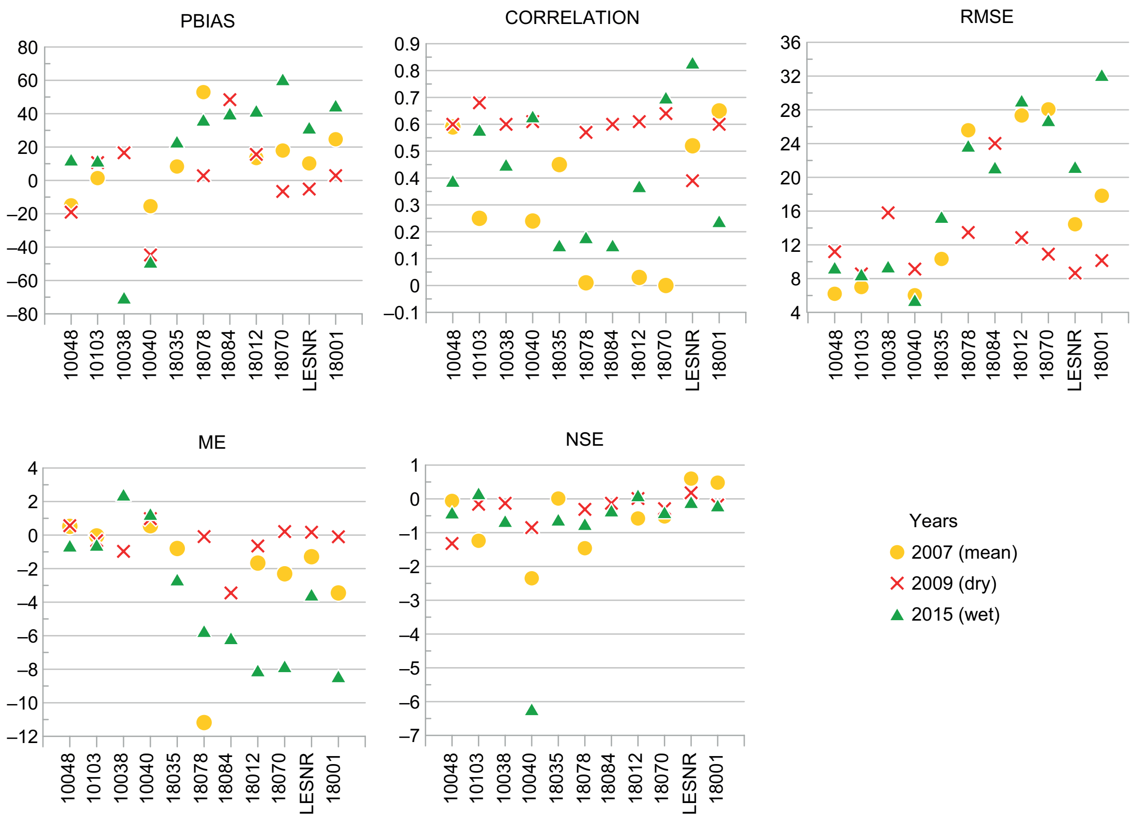

Fig. 4. Scatter plots of statistical metrics for grid to point SP estimates versus in-situ observations of maximum events in average (2007), dry (2009), and wet (2015) years. The x-axis axis marks correspond to the climatological stations' IDs shown in Fig. 1a.

For the LS correction (Fig. 6), a general reduction of PBIAS to optimal values is seen for all station points and during a wet year. In the case of 2007, only two of the locations in the upper region do not adjust correctly, and for the dry year, at the upper and lower zone an overestimation of SPP is seen. A positive correlation would be observed with the LS corrections for the dry year. For NSE, just two points in 2007 and one in 2009 coincide with the target NSE value. RMSE incremented in the lower basin points for average and wet years. ME with LS reduced to values between the range of –0.53 and 0.55 units, except for one site in the middle-lower sub-basins for the dry year.

LOCI corrections have better effects on PBIAS for 2009 and 2015 (Fig. 7) for upper and lower regions, respectively, unlike those for 2007. For all the points in the dry year, positive higher correlations appeared. Two stations with lower values for the average year, one under 150 masl in 2009 and one for the upper zone in 2015, are near the NSE of 1. Lower RMSE and ME values are spotted in the upper points; nonetheless, the range is greater than without correction.

PT reduces PBIAS in all points and climatological conditions (Fig. 8). Corrected SPP for 2007 shows medium-high positive correlations at two upper and lower stations. Correlations for the dry year are generally medium positive, and 2015 reflects lower positive values. RMSE values are higher when compared with non-corrected SPP conditions. ME values are lessened overall in the points and years studied. For NSE, PT does not reflect an important improvement.

As the aim of this project was to assess the bias of the CHIRPSv2.0 satellite precipitation product for maximum annual events based on in-situ observations at the sub-basin scale, the selection of the appropriate CT in this study was assessed not only at the point scale but also at the sub-basin scale. Therefore, the correction factors calculated for each point and method were interpolated at the sub-basin

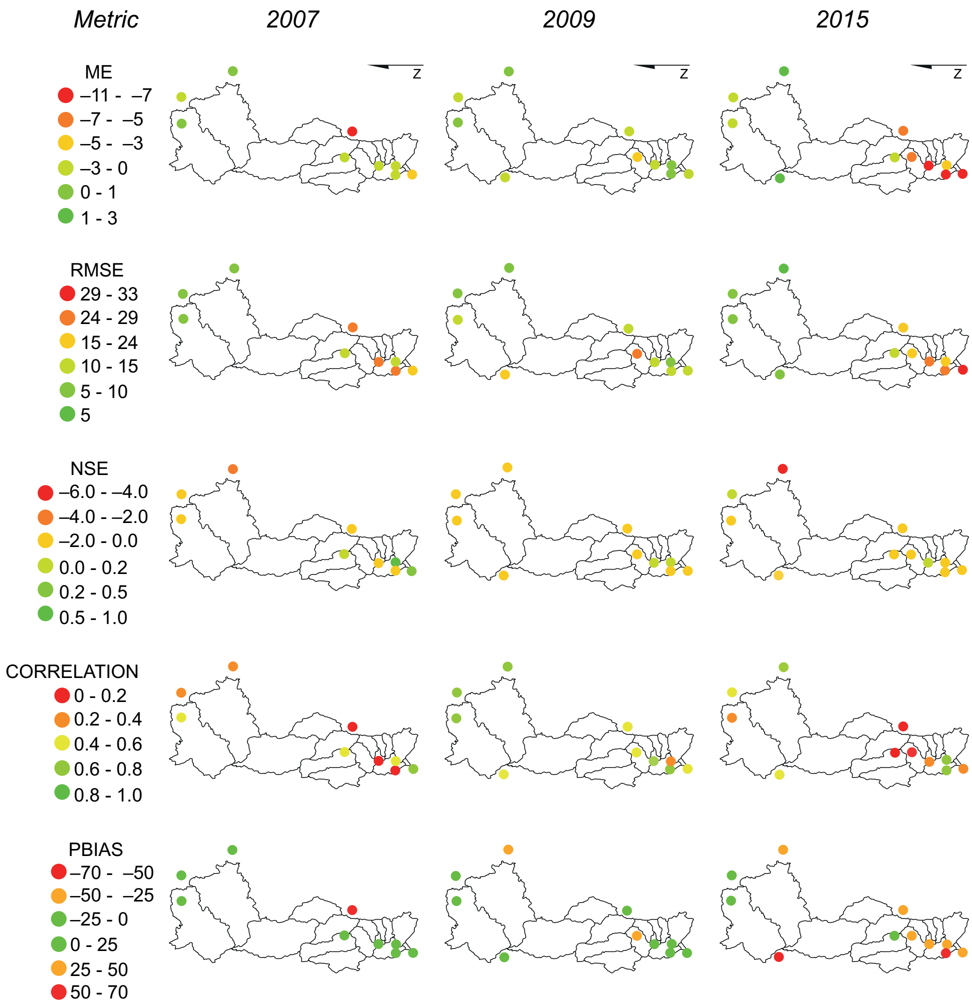

Fig. 5. Statistical metrics by precipitation gauge for satellite precipitation products (SPP) estimates vs. in-situ observations of maximum events in average (2007), dry (2009), and wet (2015) years.

scale using the Thiessen polygon and the IDW methodology (Fig. 9).

With both interpolation methods, higher values of the *sm* factors were defined for PT techniques for average and wet years and sub-basins located at the middle and upper part of the basin. Meanwhile, for the dry year (2009), the SPP must be corrected using the LOCI and LS correction factors of an order of 3.0 and 8.0 times at the middle region according to Thiessen interpolation and of 2.0 to 5.0 through IDW. For 2015, lower values of correction factors are required for LS and LOCI, and in the case of *bm* and *sm* coefficients of PT, greater CF values are needed at the lower sub-basins and middle-upper zone. Most of the values are similar in magnitude between the applied interpolation techniques. However, for LS and LOCI in 2009, CF values interpolated using the Thiessen approach were slightly higher than those obtained using IDW. This could potentially lead to an overestimation in dry conditions. Meanwhile, PT *sm* in 2007, PT *sm*, and PT *bm* for 2015 are also higher with the Thiessen method, which could lead to higher precipitation values in the wet year.

By applying CF for each interpolation method, the corrected mean daily SPP for maximum annual events for each sub-basin is estimated, and a

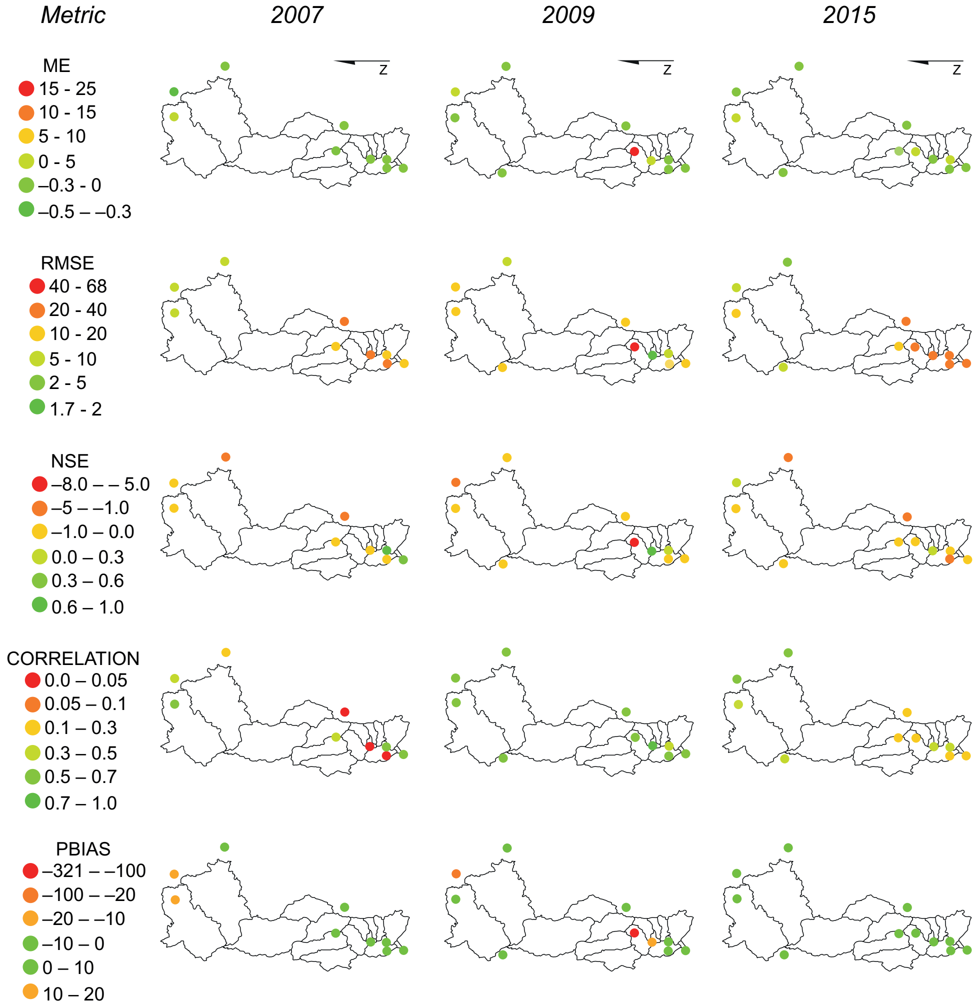

Fig. 6. Statistical metrics by precipitation gauge for linear scaling (LS) corrected satellite precipitation products (SPP) estimates vs. in-situ observations of maximum events in average (2007), dry (2009), and wet (2015) years.

comparison with the mean maximum daily observed precipitation is developed. Figures 10, 11, 12. 13, and 14 describe the behavior of the statistical metrics of corrected mean daily satellite precipitation products and observed values for maximum annual events at the sub-basin scale, with Thiessen and IDW CF interpolation.

As a mayor variability is related to the PT correction methodology for most metrics and years, the correspondent metrics are not shown in the figures to avoid overcrowding (refer to the supplementary material for details). For the remaining approaches, LOCI has a slightly lower PBIAS for wet and average years. Smaller RMSE values are estimated for 2007 and 2009 for LOCI without considering outliers and PT corrections. In the average and dry years, the correlation between corrected SPP and observed data is similar to positive medium values. In 2015, positive low correlation values are identified for LS and LOCI. Furthermore, for the periods of interest, most of the sub-basins result in NSE less than zero, with values nearest to 0 but not ideal for LOCI in 2007. The lowest values, with the least dispersion ME values for 2007, 2009, and 2015 correspond to LOCI.

A comparison of metrics at the sub-basin scale can also be analyzed in these figures. Whitin the

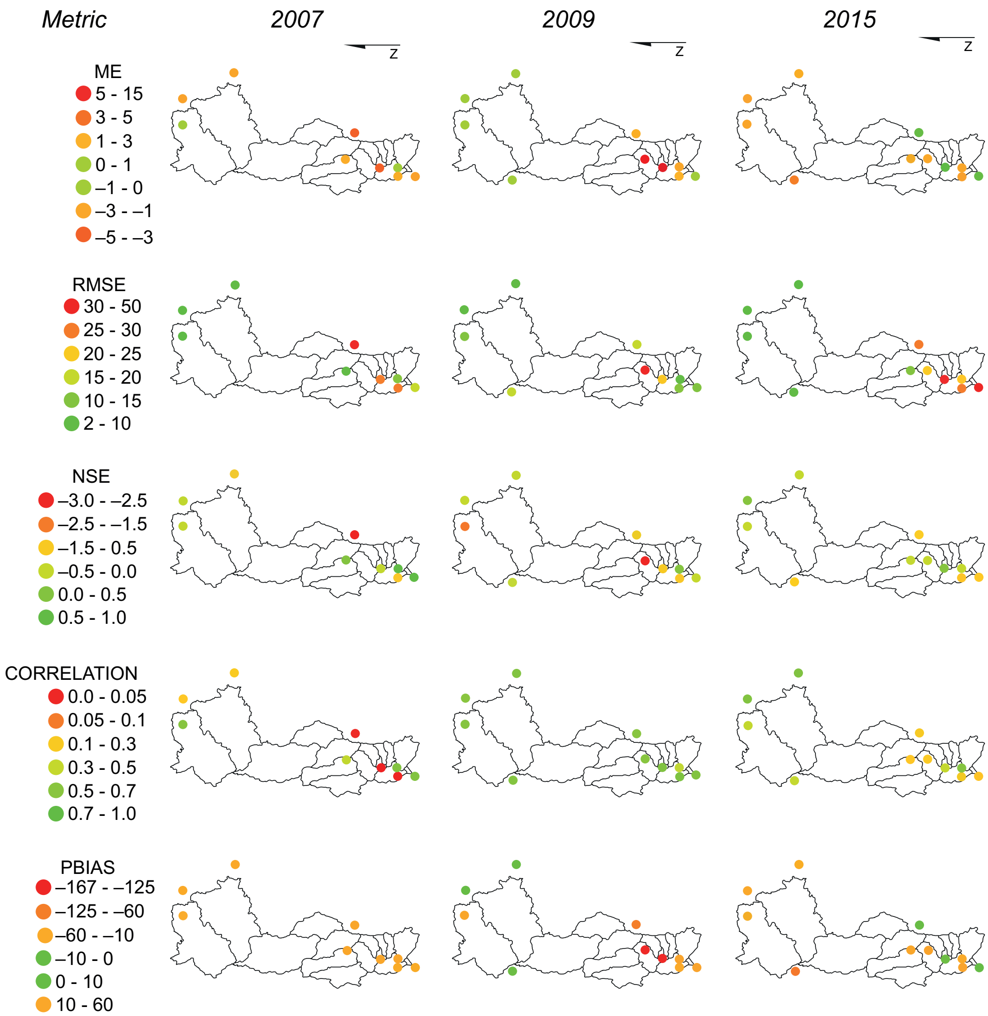

Fig. 7. Statistical metrics by precipitation gauge for local intensity scaling (LOCI) corrected satellite precipitation products (SPP) estimates vs. in-situ observations of maximum events in average (2007), dry (2009), and wet (2015) years.

studied periods, LOCI shows the smallest PBIAS for the middle basin region in 2007 and 2015. PBIAS, RMSE, ME, and NSE values for PT at the lower sub-basins can be related to an overestimation of precipitation. As expected, for 2007 and 2009 for LS and LOCI, better correlations are detected for upper and lower sub-basins, where in-situ observations are available. However, LOCI corrections reveal at least positive medium correlations overall for the sub-basins and the dry year, followed by the average scenario. Lesser ME and NSE are obtained for 2007 for LS and LOCI.

Considering PBIAS, ME, and NSE, the LOCI technique defines mean values for the sub-basins at the middle zone below the percentage established as ideal in the literature for average and wet years, with Thiessen correction factors (for PBIAS, 3.73 and –7.52%, respectively). As for the upper region, correlation is better only for the highest sub-basins in the average and dry year, with LS and LOCI; PBIAS exceeds the acceptable limits; RMSE is above 10 units and ME below this value; and NSE surpasses the optimal value of 1, except for sub-basin 1 in 2007. Addressing the sub-basins below 150 masl, medium

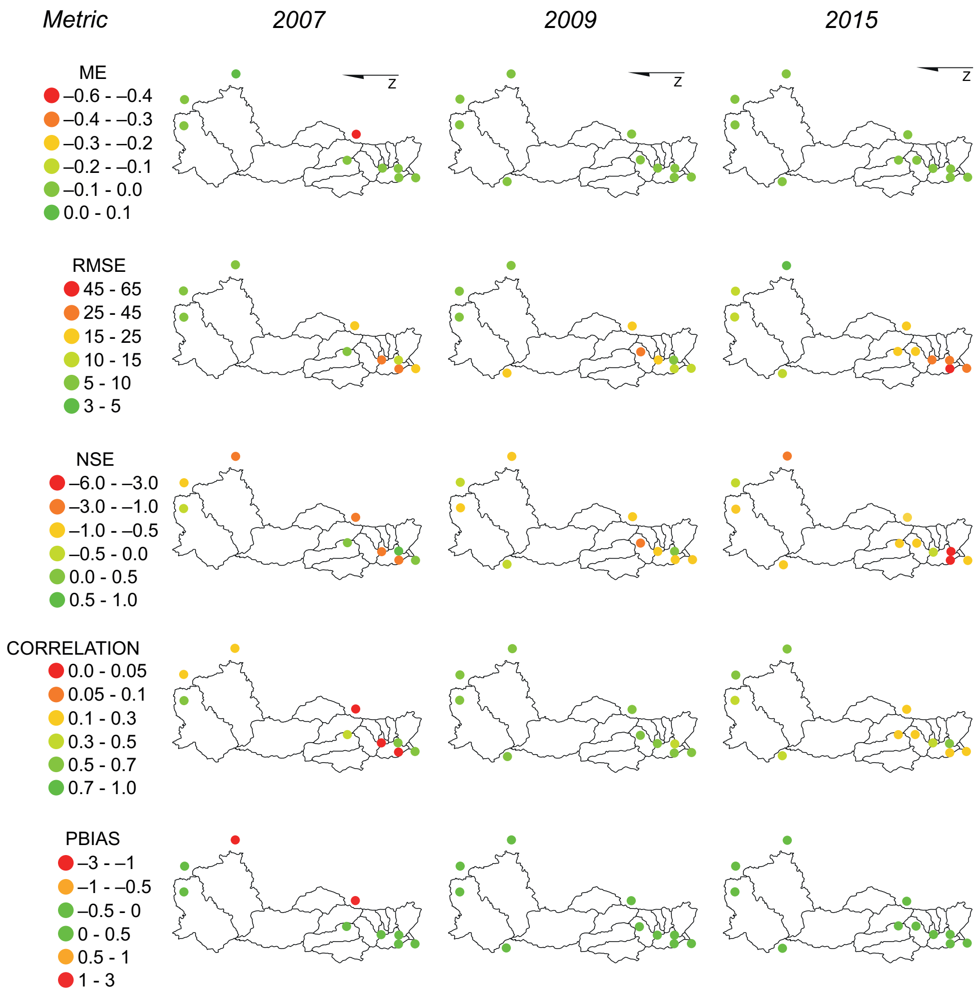

Fig. 8. Statistical metrics by precipitation gauge for power transformation (PT) corrected satellite precipitation products (SPP) estimates vs. in-situ observations of maximum events in average (2007), dry (2009), and wet (2015) years.

and high correlation values are observed; very high NSE coefficients and the applied CT led to overestimation of SPP but values of RMSE and ME WERE under 15 and 5 units, respectively.

When considering the Thiessen interpolation approach for the correction factors, LOCI seems to provide a better bias correction according to the selected statistical metrics, namely PBIAS, NSE, and ME, compared to LS and PT. Consequently, this satellite precipitation product CT is considered suitable for the conditions of maximum annual events at the Acaponeta River basin.

The maximum annual precipitation is an important variable commonly used to design storage, drainage, and flood protection infrastructure. Since the authors seek to revise the maximum annual precipitation associated with flood events in the present study, once the CT is selected, the daily mean satellite precipitation product at sub-basin scale for maximum annual events for the period 2001-2020 is bias-corrected.

Figure 15 shows the values of the observed and corrected maximum annual precipitation for each sub-basin. The corrected values result from applying the LOCI technique and correction factor interpolated with the Thiessen method. As mentioned before, the year 2011 corresponds to a generalized national drought (CONAGUA, 2012) with no records

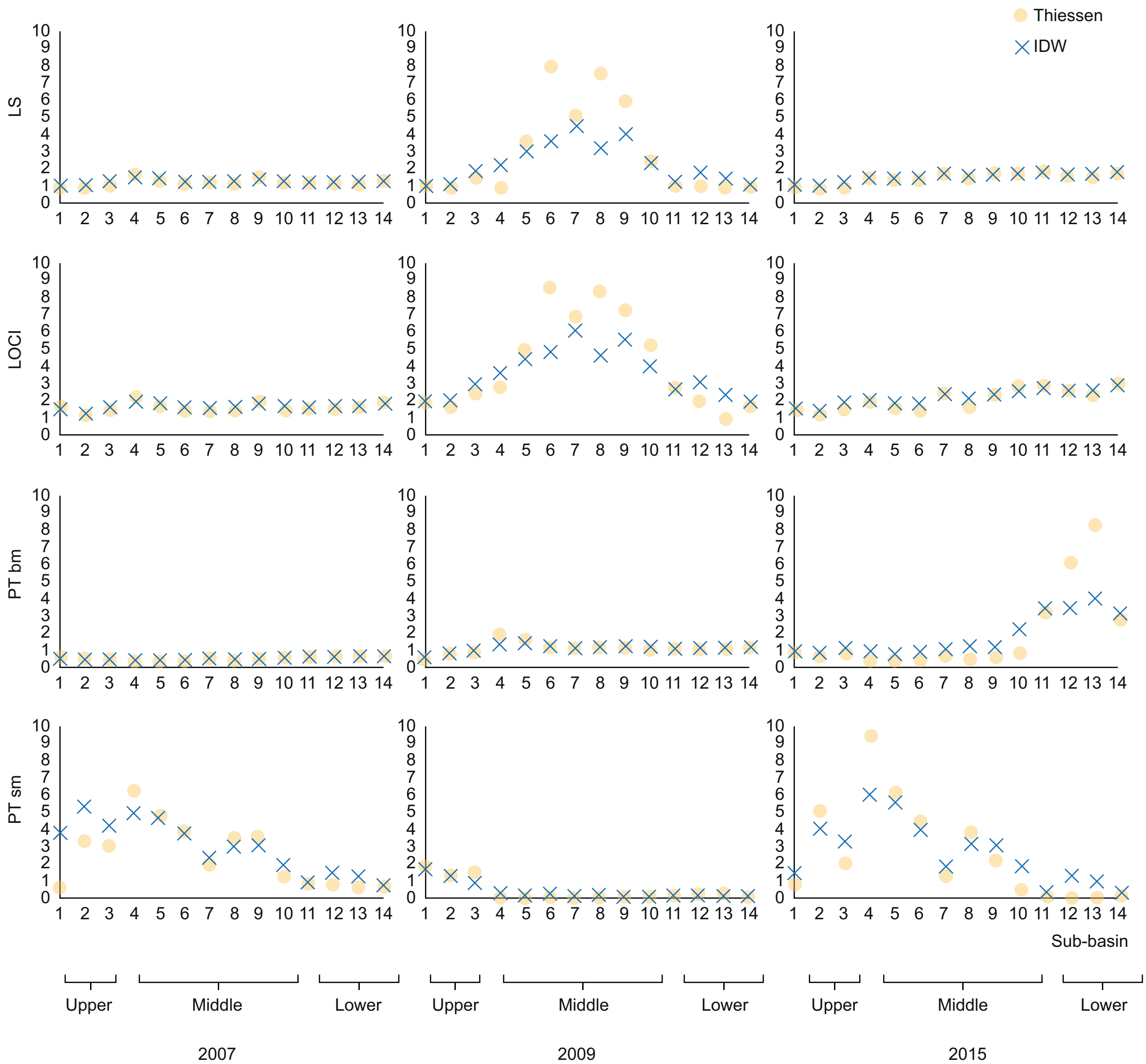

Fig. 9. Correction factors at the sub-basin scale for average (2007), dry (2009), and wet (2015) years at the sub-basin scale for the Thiessen and inverse distance weighting (IDW) interpolation methods.

available; therefore, the mean value of the correction factors for the total period of analysis was used for the correction of SPP, since using the CF of the dry year (2009) would have produced values above the wet year records.

To highlight the usefulness of this study's results and according to the objectives of this paper, a preliminary analysis was addressed through the application of the NRCS (2004) methodology. The potential direct runoff was obtained for raw and corrected SPP (shown in Figure 16) for each sub-basin and temporal scenario, according to the physiographic, climatological, and land use conditions (see the supplementary material).

4. Discussion

The outcomes of this study allow us to assess the differences between OP and SPP at grid to point scale by performing a spatiotemporal analysis of the available

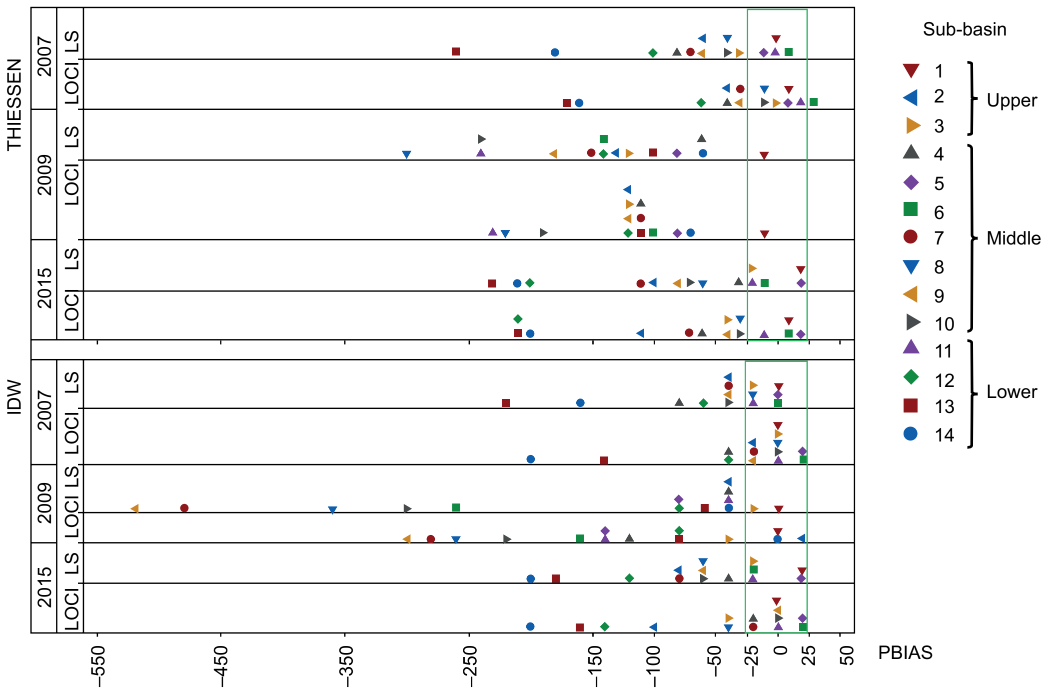

Fig. 10. Dots plots of percentual bias (PBIAS) for linear scaling (LS) and local intensity scaling (LOCI) corrected satellite precipitation products (SPP) estimates vs. in-situ observations of maximum events in average (2007), dry (2009), and wet (2015) years.

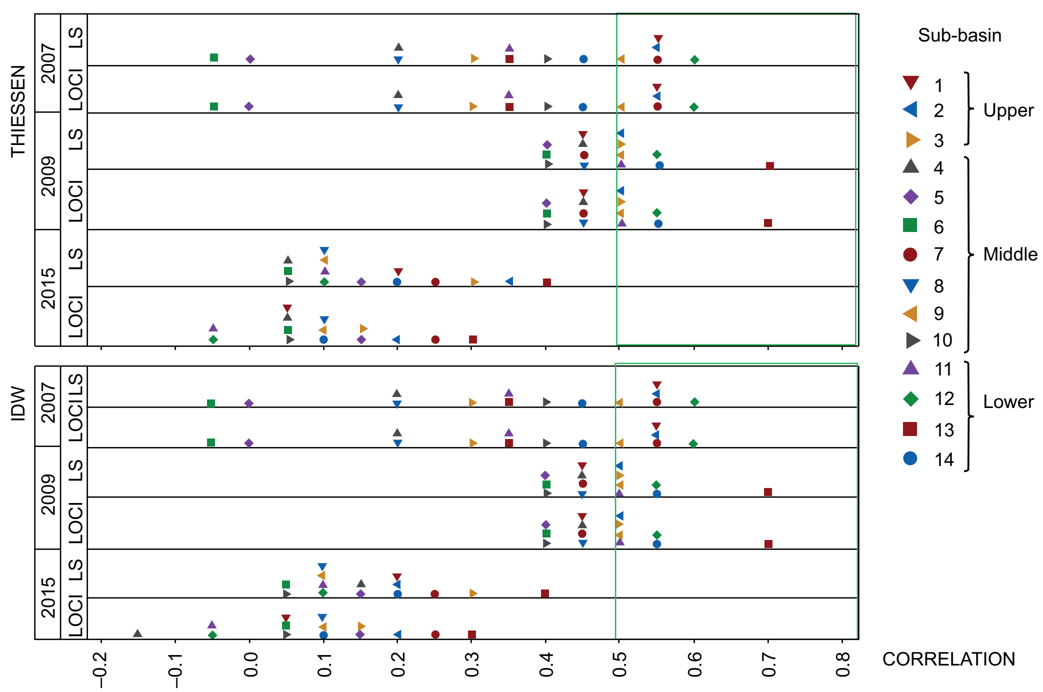

Fig. 11. Dots plots of correlation for linear scaling (LS) and local intensity scaling (LOCI) corrected satellite precipitation products (SPP) estimates vs. in-situ observations of maximum events in average (2007), dry (2009), and wet (2015) years.

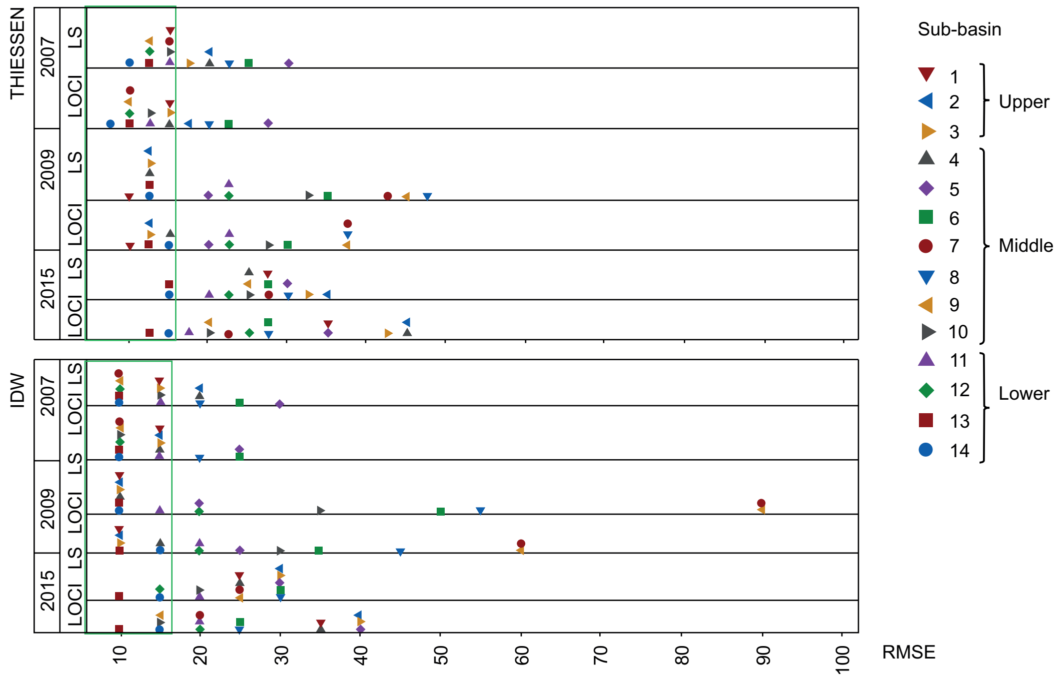

Fig. 12. Dots plots of root mean square error (RMSE) for linear scaling (LS) and local intensity scaling (LOCI) corrected satellite precipitation products (SPP) estimates vs. in-situ observations of maximum events in average (2007), dry (2009), and wet (2015) years.

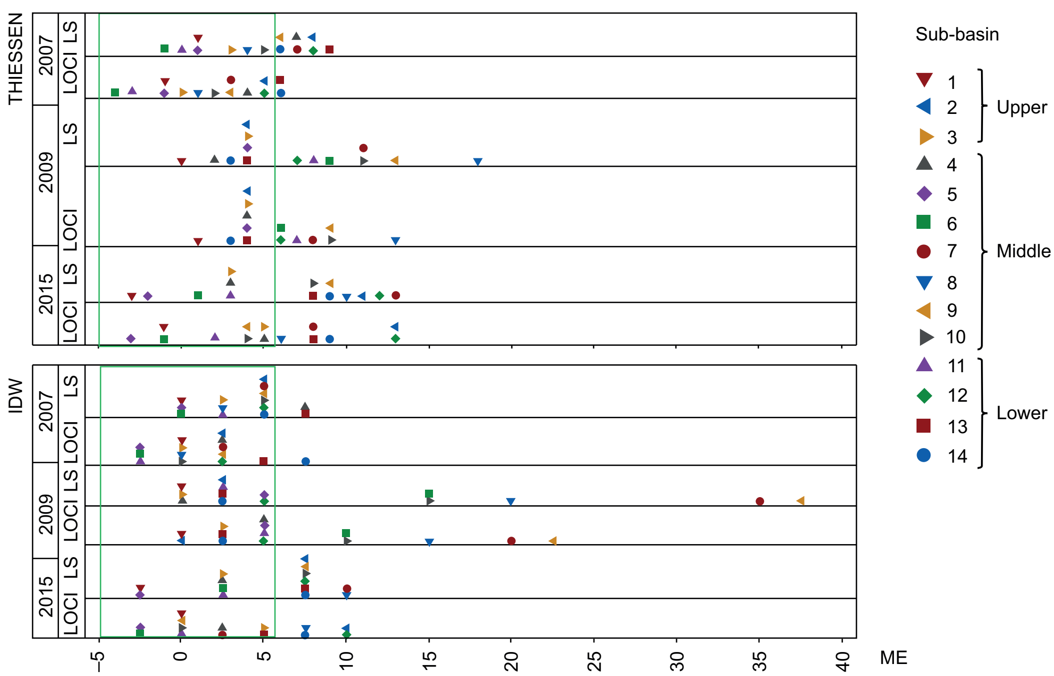

Fig. 13. Dots plots of mean error (ME) for linear scaling (LS) and local intensity scaling (LOCI) corrected satellite precipitation products (SPP) estimates vs. observations of maximum events in average (2007), dry (2009), and wet (2015) years.

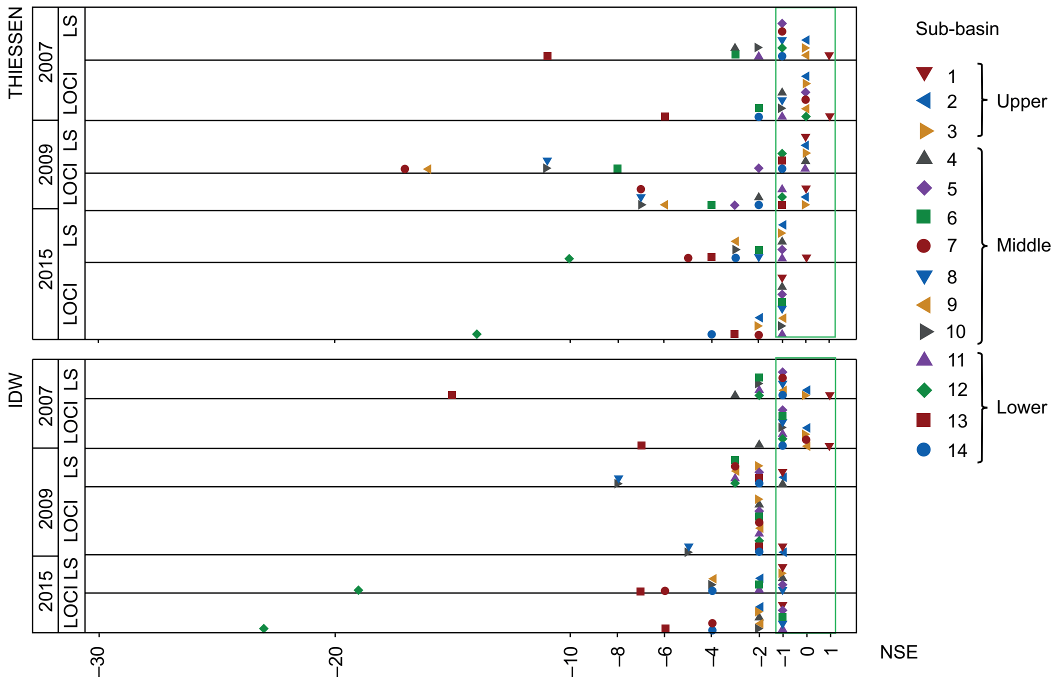

Fig. 14. Dots plots of Nash-Sutcliffe efficiency coefficient (NSE) for linear scaling (LS) and local intensity scaling (LOCI) corrected satellite precipitation products (SPP) estimates vs. in-situ observations of maximum events in average (2007), dry (2009), and wet (2015) years.

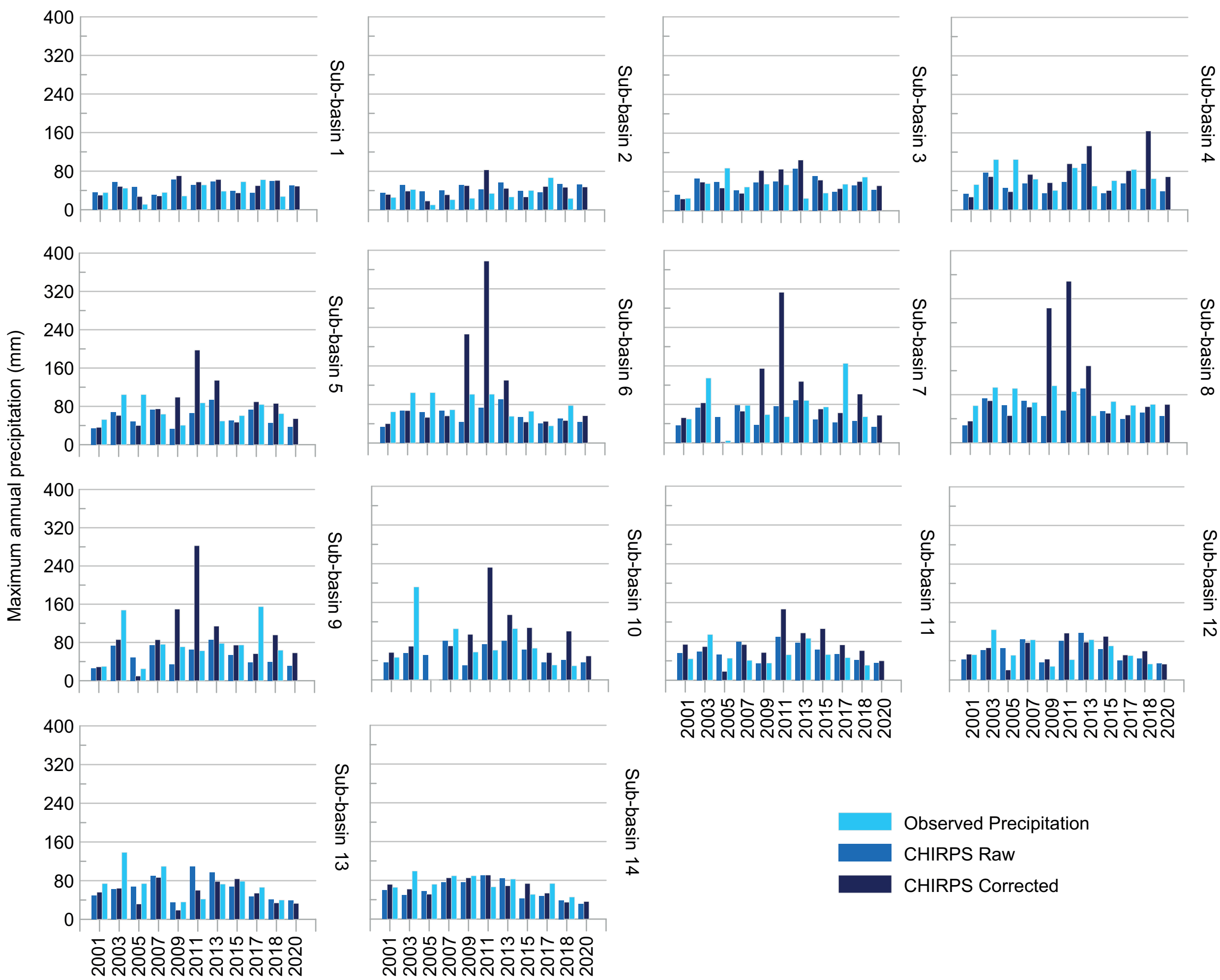

Fig. 15. Observed, raw, and corrected Climate Hazards Group Infrared Precipitation with Station (CHIRPS) product average annual maximum precipitation at sub-basin scale from 2001-2020.

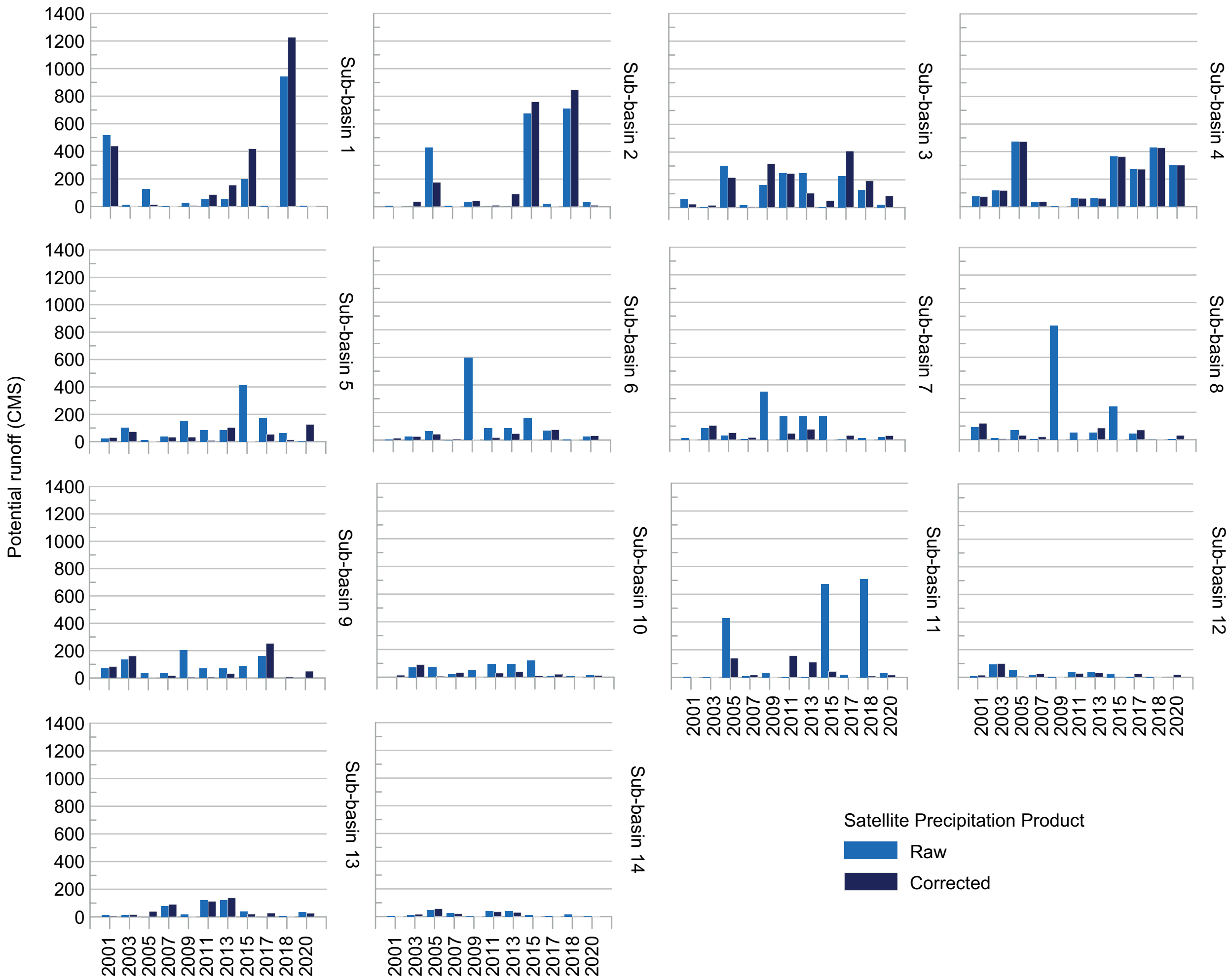

Fig. 16. Estimated potential direct runoff at sub-basin scale with raw and corrected maximum annual satellite precipitation for 2001-2020.

SPP with respect to scarce in-situ observations for dry, average, and wet climatological conditions. As well as determine the appropriate CT at sub-basin scale and improve the satellite precipitation product for maximum annual events for a given period, which can be used as the input for hydrological analysis of extreme hydrometeorological events such as floods.

Previous works (Fang et al., 2015; Bhatti et al., 2016; Velásquez et al., 2020; Belayneh et al., 2020; Soo et al., 2020; Aksu et al., 2022, 2023; González-Ortigoza et al., 2023; Ceferino-Hernández et al., 2024) have successfully corrected SPP from different sources by utilizing not only the bias CTs employed in this paper, but also another that requires more data processing. Moreover, preceding uses of these techniques commonly had approaches for broader temporal and spatial scales since they were not intended for examining short climatological events such as extreme precipitations and flood events (Saber and Yilmaz, 2018; Soo et al., 2020; Villate et al., 2023), but fewer studies have been identified on the application of bias correction techniques for a Mexican basin at the sub-basin scale (Dawa et al. 2024).

Since in this work, the lack of observed precipitation data is identified, particularly for the middle basin, and as the study of maximum annual precipitation events would require the correction of SPP for several years, it results useful to develop a methodology that, with the revision of dry, average and wet years, allows the selection of an adequate CT according to the conditions of the basin of interest, especially to the regions that have scarce data. Regarding the interpolation methods applied to correction factors, in general, similar values were obtained for the average year, LS, and LOCI; for 2015, a greater CF was estimated for LOCI IDW, and for the dry year, the Thiessen approach projected a higher CF for the middle sub-basins. Particularly for the PT parameters and wet year, there are considerable differences between the Thiessen and IDW methods.

Considering the topographic configuration and evaluation of bias, the points at the middle and lower region present higher PBIAS, RMSE, and ME, while the upper section of the Acaponeta basin showed lower PBIAS and RMSE. Small positive correlations are observed in the middle zone, coinciding with the lack of observed precipitation. Lastly, NSE values were greater in the upper and middle regions. The obtained PBIAS values for raw satellite precipitation data are similar to those shown in the literature on extreme precipitation events in Mexico (Mayor et al., 2017; Saber and Yilmaz, 2018; Villate et al., 2023). Regarding the topographic regions of the basin, unlike the findings of Aksu and Akgül (2020) and Yeh et al. (2020), PBIAS values are lower at higher elevations in the case of the dry year, while for mean and wet scenarios, moderate and higher values are observed in lower elevations. Moreover, at the point to grid-scale, PBIAS values show an analogous behavior to those calculated by Akgül and Aksu (2021). As for RMSE, Villate et al. (2023) analyzed a region near the study case with comparable values. As identified in the literature, a better correlation (Saber and Yilmaz, 2018) between in-situ observations and SPP is identified for dry conditions, and in the case of a wet scenario, only four upper and lower region points accounted for similar values of correlation. The NSE values for dry conditions correspond to the ones presented by Saber and Yilmaz (2018) and are below those obtained by Akgül and Aksu (2021).

Once the CTs were applied at the point scale, the PT method corrected PBIAS generally to ± 3%. It produced a moderate to high positive correlation for dry and average years, especially at the upper and lower regions. The correlations are similar to those obtained at a daily temporal scale by Kagone et al. (2023). PBIAS was generally eliminated for 2015 with LS; in 2007 and 2009, the adjustment of the upper zone was not optimal. LOCI corrected PBIAS, ideally for the middle and lower areas. With respect to the correlation, positive values were obtained for LS and LOCI in the dry year. At the lower section of the basin, RMSE increased with LS for average and wet years. RMSE and ME resulted in higher values than without LOCI correction. According to the topographic regions, in the analysis of Luo et al. (2020), LS and PT generate lower ME values at the middle and lower regions of their case study, and LOCI increases with elevation, an aspect that for the Acaponeta upper sub-basins, coincides in the case of the mean year (2007).

At the sub-basin scale, the performance of CT differs from the previous results of this study at the point scale, similarly as observed by Bai et al. (2018) from a comparison between evaluation at the point and grid scale. Regarding PBIAS, only LOCI generated values under the accepted limits for average and wet years at the middle zone, and the remaining techniques produced PBIAS over the defined range, specifically with PT. Through all the CT, small positive correlations were observed for 2007 and 2009 in the middle and lower areas, while the upper region showed medium-high positive correlations only for 2009. RMSE values below 15 units were recorded for LS and LOCI in average and dry years at the upper and lower sub-basins, respectively. For the mean error using LS and LOCI, average and wet years in the middle and lower zones relate to values under five units, unlike dry years, when a better performance is observed. In the case of PT, ME is above five units in all scenarios. With LS, LOCI, and PT, NSE points to an inferior performance of these methodologies to correct the satellite precipitation product. As established by Fang et al. (2015), LS and LOCI perform better than PT for bias correction, in this case, at a sub-basin scale. Among the two possible interpolation methods of the correction factors, the Thiessen interpolation approach of the CF for the LOCI method better approximates the SPP, especially in the sub-basins of the central region where there is a lack of precipitation measurements.

Over time, there is an increase in the adjusted values of maximum annual precipitation for the upper sub-basins, which is reflected in the potential direct runoff. Nevertheless, for the middle region, four of the seven sub-basins showed a tendency to lower maximum precipitation and potential direct runoff. Overall, the lower basin presents a reduction in total maximum precipitation and the resulting direct runoff, with the exception of sub-basin 11. After the correction, regarding the observed data at the sub-basin scale, differences were still expected for some dry and wet years in the middle zone, where there is a lack of in-situ observations.

From the preliminary estimation of the potential direct runoff calculated with the NRCS method at a sub-basin scale, the effect of raw and corrected SPP was identified in the case of scarce observed data. In general, the impact of the corrected SPP in the generated direct runoff is more visible in the middle sub-basins with increments, followed by the lower sub-basins. As for the upper region, it resulted in a decrease in the runoff. With the use of corrected SPP, it was possible to calculate the direct runoff at a smaller spatial scale, especially for the middle region of the basin, where the runoff estimation with the little-observed information would be a complex process and might be associated with more uncertainty. From these preliminary results, more accurate hydrological analysis can be developed and calibrated; nevertheless, those processes are out of the scope of the present study.

In addition, this paper provides a spatial assessment of SPP bias, considering the location of the in-situ observations and their elevation, which have previously been associated with bias in the literature. By estimating the bias at a sub-basin scale, more detailed hydrological and flood analysis can be approached, and by detecting the zones prone to bias for satellite precipitation products at a basin or sub-basin scale, the decision to place new climatological stations could be supported. Nevertheless, the present study faces limitations regarding the scarce and spatially well-distributed observed precipitation at the studied basin scale, which could be related to the statistical metrics values that describe bias before and after the application of CTs.

5. Conclusions

Satellite estimates emerge as a suitable option for performing hydrological studies to cope with scarcely observed precipitation records, mainly oriented to flood exposure analysis and management. However, the origin and corroboration of these estimates could result in considerable bias, along with the under- and over-estimation of runoffs used for the different water security dimensions, including flood and drought management. With this project, the authors looked forward to assessing the bias of the CHIRPSv2.0 satellite precipitation product for maximum annual events and at a sub-basin scale and to select an appropriate CT applied to enhance rainfall estimates corresponding to the annual maxima of the period 2001-2020 for the Acaponeta River basin, near the Mexican Pacific Ocean.

It was possible to evaluate and substantially correct the existing bias for maximum annual events through the application of the proposed methodology, considering different climatological conditions not only at grid to point scale, but for each of the sub-basins of interest, considering their location within the topographic configuration of the basin. By subdividing the total basin area and analyzing its topographic characteristics, it was possible to represent better the governing hydrological processes, which allows the definition of the spatial distribution of climatological conditions, as estimated by the satellite precipitation product, and the contribution of each sub-basin to runoff generation.

Moreover, differences in the performance of the correction methods were identified between the point and sub-basin scales that can be associated with the limited measurement points and the interpolation procedures. Even though PT had a good performance at the point scale, for the sub-basins, PBIAS resulted in large ranges of overestimation at the upper zone for the average and dry years, while for the lower part, it behaved similarly for the wet year. Although good bias reduction at the precipitation gauge points was observed with LS and LOCI generally, at the sub-basin scale, LS overestimated for all regions. LOCI showed better SPP PBIAS corrections in the middle and lower zones for the mean year, in the upper and middle regions for the wet year, and a greater range of overestimation in the upper sub-basins for the average and all the sub-basins in the dry year.

From the findings of this study, it was possible to document the degree of bias correction of SPP with regard to OP through different statistical metrics and determine which of the CTs used performs best at the point or sub-basin scale. The influence of the spatial location and elevation of the measurements, as well as different climatological conditions, can also be related.

With the presented methodology, some practical implications can be recognized, like the acknowledgment of the existing bias of estimated and measured maximum annual precipitation events and the definition of a suitable CT according to the climatological and physiographic characteristics of the several regions of a basin. The importance of the research lies in using and improving the available estimated precipitation to fill the gap of this climatological variable in historical records, which is the main input of hydrological studies. In the context of extreme hydrometeorological events, by correcting the maximum annual precipitation database, hydrological studies can be developed for infrastructure design and flood risk management, reducing under- or over-estimating records that can result in economic losses. As a preliminary attempt to address the latter, the potential direct runoff was estimated with raw and corrected SPP, and it was found that with corrected SPP, the runoff of the middle region would increase. Ongoing research is exploring the use of corrected satellite precipitation products to analyze the evolution of the hydrological and hydraulic response to extreme events. The results of these in-progress studies will provide further evidence of the applicability of SPP in hydrological analysis, particularly for flood assessment.

To better analyze and reduce SPP bias in general, accurate and sufficient measured precipitation data, at specific temporary and spatial scales, to represent the behavior of this variable distributed at a basin scale, is required. A call for proper engagement in terms of better precipitation monitoring data is necessary to improve the assessment of extreme hydrometeorological events, contributing to the knowledge of flood risk. However, this paper provides a way to develop a more detailed semi-distributed rainfall record of annual maxima at a sub-basin scale using the scarce observed and available rainfall data coupled with a high-resolution global database. The result of this approach is one of the essential variables for hydrological analysis and can be useful for studies developed by local, regional, and national institutions for water management of the different climatological conditions to which basins are exposed at different spatial scales.

Acknowledgments

The authors thank the Universidad de las Américas Puebla and CONAHCYT for all the support and facilities provided to carry out this work. UC Alianza MX strategic grant IRGUCMX2021-02 facilitated the interaction and collaboration between authors. Special thanks to Professor Carlos Patiño-Gómez (†) for his invaluable mentoring and participation in this paper. The authors also thank Dr. Benito Corona-Vásquez for his contribution to the preparation of this paper.

References

Adhikari A, Behrangi A. 2022. Assessment of satellite precipitation products in relation with orographic enhancement over the western United States. Earth and Space Science 9: e2021EA001906. https://doi.org/10.1029/2021EA001906

Akgül MA, Aksu H. 2021. Areal precipitation estimation using satellite derived rainfall data over an irrigation area. Turkish Journal of Agriculture - Food Science and Technology 9: 386-394. https://doi.org/10.24925/turjaf.v9i2.386-394.4061

Aksu H, Akgül MA. 2020. Performance evaluation of CHIRPS satellite precipitation estimates over Turkey. Theoretical and Applied Climatology 142: 71-84. https://doi.org/10.1007/s00704-020-03301-5

Aksu H, Cavus Y, Aksoy H, Akgul MA, Turker S, Eris E. 2022. Spatiotemporal analysis of drought by CHIRPS precipitation estimates. Theoretical and Applied Climatology 148: 517-529. https://doi.org/10.1007/s00704-022-03960-6

Aksu H, Yaldiz SG, Taflan GY, Akgül MA. 2023. Frequency analysis based on peaks-over-threshold approach for GPM IMERG precipitation product. Theoretical and Applied Climatology 154: 275-289. https://doi.org/10.1007/s00704-023-04555-5

Ávila-Carrasco JR, Júnez-Ferreira HE, Gowda PH, Steiner JL, Moriasi DN, Starks PJ, González J, Villalobos AA, Bautista-Capetillo C. 2018. Evaluation of satellite-derived rainfall data for multiple physio-climatic regions in the Santiago River basin, Mexico. Journal of the American Water Resources Association 54: 1068-1086. https://doi.org/10.1111/1752-1688.12672

Báez-Villanueva OM, Zambrano-Bigiarini M, Ribbe L, Nauditt A, Giraldo-Osorio JD, Thinh NX. 2018. Temporal and spatial evaluation of satellite rainfall estimates over different regions in Latin-America. Atmospheric Research 213: 34-50. https://doi.org/10.1016/j.atmosres.2018.05.011

Bai L, Shi C, Li L, Yang Y, Wu J. 2018. Accuracy of CHIRPS satellite-rainfall products over mainland China. Remote Sensing 10: 362. https://doi.org/10.3390/rs10030362

Belayneh A, Sintayehu G, Gedam K, Muluken T. 2020. Evaluation of satellite precipitation products using HEC-HMS model. Modeling Earth Systems and Environment 6: 2015-2032. https://doi.org/10.1007/s40808-020-00792-z

Bhatti HA, Rientjes T, Haile AT, Habib E, Verhoef W. 2016. Evaluation of bias correction method for satellite-based rainfall data. Sensors 16: 884. https://doi.org/10.3390/s16060884

Bruster-Flores JL, Ortiz-Gómez R, Ferriño-Fierro AL, Guerra-Cobián VH, Burgos-Flores D, Lizárraga-Mendiola LG. 2019. Evaluation of precipitation estimates CMORPH-CRT on regions of Mexico with different climates. Water 11: 1722. https://doi.org/10.3390/w11081722

Ceferino-Hernández L, Magaña-Hernández F, Campos-Campos E, Morosanu GA, Torres-Aguilar CE, Mora-Ortiz, Díaz SA. 2024. Assessment of PERSIANN satellite products over the Tulijá River basin, Mexico. Remote Sensing 16: 2596. https://doi.org/10.3390/rs16142596

CENAPRED. 2021. Inundaciones históricas a nivel nacional. Atlas nacional de riesgos hidrometeorológicos, inundaciones, históricos. Centro Nacional de Prevención de Desastres, Mexico. Available at: http://www.atlasnacionalderiesgos.gob.mx/portal/fenomenos/ (accessed 2022 March 15)

CENAPRED. 2022. Impacto socioeconómico de los principales desastres ocurridos en México. Resumen ejecutivo 2021. Centro Nacional de Prevención de Desastres, Mexico. Available at: https://www.cenapred.gob.mx/es/Publicaciones/archivos/487-RESUMENEJECUTIVOIMPACTO2021.PDF (accessed 2023 June 3)

CENAPRED. 2023. Impacto socioeconómico de los principales desastres ocurridos en México. Resumen ejecutivo 2022. Centro Nacional de Prevención de Desastres, Mexico. Available at: https://www.cenapred.unam.mx/es/Publicaciones/archivos/494-RESUMENEJECUTIVOIMPACTO2022.pdf (accessed 2023 September 4)

Chen H, Sun L, Cifelli R, Xie P. 2022. Deep learning for bias correction of satellite retrievals of orographic precipitation. IEEE Transactions on Geoscience and Remote Sensing 60: 4104611. https://doi.org/10.1109/TGRS.2021.3105438

CICESE. 2022. Base de datos climatología nacional (sistema CLICOM). Centro de Investigación Científica y de Educación Superior de Ensenada, BC, Mexico. Available at: https://www.cicese.edu.mx/ (accessed 2023 January 9)

CONABIO. 1998. Climas. Portal de geoinformación 2023. Comisión Nacional para el Conocimiento y Uso de la Biodiversidad, Mexico. Available at: http://www.conabio.gob.mx/informacion/gis/?vns=gis_root/clima/climas/clima1mgw (accessed 2023 October 23)

CONAGUA. 2012. La evolución de la sequía en México en 2011. Comisión Nacional del Agua, Servicio Meteorológico Nacional, Mexico. Available at: https://www.inegi.org.mx/contenidos/eventos/2012/sequias/P1_004-05AdelinaAlbanilyReynaldoPascual.pdf (accessed 2022 June 15)

CONAGUA. 2019. Sistema de Información Hidrológica (SIH). Comisión Nacional del Agua, Mexico. Available at: https://sih.conagua.gob.mx/ (accessed 2021 June 13)

CONAGUA. 2023. Distribución de la precipitación normal. Sistema Nacional de Información del Agua, situación de los recursos hídricos, precipitación. Comisión Nacional del Agua, Mexico. Available at: https://sinav30.conagua.gob.mx:8080/SINA/ (accessed 2023 June 13)

Dawa SY, Tan ML, Samat N, Roy R, Zhang F. 2024. Evaluation of five gridded precipitation products for estimating precipitation and drought over Yobe, Nigeria. Water Supply 24: 2039-2054. https://doi.org/10.2166/ws.2024.113

De Jesús A, Breña-Naranjo JA, Pedrozo-Acuña A, Alcocer Yamanaka VH. 2016. The use of TRMM 3B42 product for drought monitoring in Mexico. Water 8: 325. https://doi.org/10.3390/w8080325

Derin Y, Yilmaz KK. 2014. Evaluation of multiple satellite-based precipitation products over complex topography. Journal of Hydrometeorology 15: 1498-1516. https://doi.org/10.1175/JHM-D-13-0191.1

Du H, Tan ML, Zhang F, Chun KP, Li L, Kabir MH. 2024. Evaluating the effectiveness of CHIRPS data for hydroclimatic studies. Theoretical and Applied Climatology 155: 1519-1539. https://doi.org/10.1007/s00704-023-04721-9

Fang GH, Yang J, Chen YN, Zammit C. 2015. Comparing bias correction methods in downscaling meteorological variables for a hydrologic impact study in an arid area in China. Hydrology and Earth System Sciences 19: 2547-2559. https://doi.org/10.5194/hess-19-2547-2015

Funk C, Peterson P, Landsfeld M, Pedreros D, Verdin J, Shukla S, Husak G, Rowland J, Harrison L, Hoell A, Michaelsen J. 2015. The climate hazards infrared precipitation with stations – A new environmental record for monitoring extremes. Scientific Data 2: 150066. https://doi.org/10.1038/sdata.2015.66

González-Ortigoza S, Hernández-Espriú A, Arciniega-Esparza S. 2023. Regional modeling of groundwater recharge in the Basin of Mexico: New insights from satellite observations and global data sources. Hydrogeology Journal 31: 1971-1990. https://doi.org/10.1007/s10040-023-02667-w

Goshime DW, Absi R, Haile AT, Ledésert B, Rientjes T. 2020. Bias-corrected CHIRP satellite rainfall for water level simulation, Lake Ziway, Ethiopia. Journal of Hydrologic Engineering 25: 05020024. https://doi.org/10.1061/(ASCE)HE.1943-5584.0001965

Huang YC, Lin YL. 2014. A study on the structure and precipitation of Morakot (2009) induced by the Central Mountain Range of Taiwan. Meteorology and Atmospheric Physics 123: 115-141. https://doi.org/10.1007/s00703-013-0290-4

INEGI. 2007. Conjunto de datos vectoriales, escala 1:1000000 Temperatura media anual. Instituto Nacional de Estadística y Geografía, Aguascalientes, Mexico. Available at: https://www.inegi.org.mx/app/biblioteca/ficha.html?upc=702825267568 (accessed 2023 October 23)

JAXA. 2010. Advanced Land Observing Satellite. Japan Aerospace Exploration Agency, Tokyo, Japan. Available at: https://www.eorc.jaxa.jp/ALOS/en/index_e.htm (accessed 2023 June 10)

Kagone S, Velpuri NM, Khand K, Senay GB, van der Valk MR, Goode DJ, Abu Hantash S, Al-Momani TM, Momejian N, Eggleston JR. 2023. Satellite precipitation bias estimation and correction using in situ observations and climatology isohyets for the MENA region. Journal of Arid Environments 215: 105010. https://doi.org/10.1016/j.jaridenv.2023.105010

Kite GW, Kouwen N. 1992. Watershed modeling using land classifications. Water Resources Research 28: 3193-3200. https://doi.org/10.1029/92WR01819

Lafon T, Dadson S, Buys G, Prudhomme C. 2013. Bias correction of daily precipitation simulated by a regional climate model: A comparison of methods. International Journal of Climatology 33: 1367-1381. https://doi.org/10.1002/joc.3518

Luo X, Fan X, Li Y, Ji X. 2020. Bias correction of a gauge-based gridded product to improve extreme precipitation analysis in the Yarlung Tsangpo-Brahmaputra River basin. Natural Hazards and Earth System Sciences 20: 2243-2254. https://doi.org/10.5194/nhess-20-2243-2020

Mayor YG, Tereshchenko I, Fonseca-Hernández M, Pantoja DA, Montes JM. 2017. Evaluation of error in IMERG precipitation estimates under different topographic conditions and temporal scales over Mexico. Remote Sensing 9: 503. https://doi.org/10.3390/rs9050503

Mendoza Uribe I. 2019. Desempeño del algoritmo RRQPE del satélite GOES 16 para la estimación de lluvia en el estado de Nayarit tras el paso del huracán Willa. Ingeniería, Revista Académica de la Facultad de Ingeniería, Universidad Autónoma de Yucatán 23: 37-51.

Mijares-Fajardo R, Lobato-Sánchez R, Patiño-Gómez C, Guevara-Polo DE. 2024. Atlantic and Pacific sea surface temperature correlations with precipitation over northern Mexico. Atmósfera 38: 217-234. https://doi.org/10.20937/ATM.53257

Morales-Velázquez MI, Herrera G del S, Aparicio J, Rafieeinasab A, Lobato-Sánchez R. 2021. Evaluating reanalysis and satellite-based precipitation at regional scale: A case study in southern Mexico. Atmósfera 34: 189-206. https://doi.org/10.20937/ATM.52789

Nakkazi MT, Sempewo JI, Tumutungire MD, Byakatonda J. 2022. Performance evaluation of CFSR, MERRA-2 and TRMM3B42 data sets in simulating river discharge of data-scarce tropical catchments: A case study of Manafwa, Uganda. Journal of Water and Climate Change 13: 522-541. https://doi.org/10.2166/wcc.2021.174

Nigussie AB, Tenfie HW, Zimale FA, Endalew A, Wudiye G. 2023. Evaluation of multiple bias correction methods with different satellite rainfall products in the Main Beles Watershed, Upper Blue Nile (Abbay) basin, Ethiopia. Journal of Water and Climate Change 14: 156-174. https://doi.org/10.2166/wcc.2022.244

NOAA. 2023. Weather glossary. JetStream – An online school for weather. National Oceanic and Atmospheric Administration, Washington DC, USA. https://www.

noaa.gov/jetstream/appendix/weather-glossary (accessed 2023 October 23)

NRCS. 2004. Estimation of direct runoff from storm rainfall. In: National engineering handbook. Natural Resources Conservation Service, Washington DC, U.S. Department of Agriculture.

Ocampo-Marulanda C, Fernández-Álvarez C, Cerón WL, Canchala T, Carvajal-Escobar Y, Alfonso-Morales W. 2022. A spatiotemporal assessment of the high-resolution CHIRPS rainfall dataset in southwestern Colombia using combined principal component analysis. Ain Shams Engineering Journal 13: 101739. https://doi.org/10.1016/j.asej.2022.101739

Perdigón-Morales J, Romero-Centeno R, Ordóñez Pérez P, Barrett BS. 2018. The midsummer drought in Mexico: Perspectives on duration and intensity from the CHIRPS precipitation database. International Journal of Climatology 38: 2174-2186. https://doi.org/10.1002/joc.5322

Roque Quiroz RA. 2023. Validación de la data de precipitación (1981-2016) del producto PISCO v2.1: Estación meteorológica, elevación, estacionalidad del año y región climática en la cuenca Tumbes, Perú. Manglar 20: 41-50. https://doi.org/10.57188/manglar.2023.005

Saber M, Yilmaz KK. 2018. Evaluation and bias correction of satellite-based rainfall estimates for modelling flash floods over the Mediterranean region: Application to Karpuz River basin, Turkey. Water 10: 657. https://doi.org/10.3390/w10050657

Schmidli J, Frei C, Vidale PL. 2006. Downscaling from GCM precipitation: A benchmark for dynamical and statistical downscaling methods. International Journal of Climatology 26: 679-689. https://doi.org/10.1002/joc.1287

Soo EZX, Wan Jaafar WZ, Lai SH, Othman F, Elshafie A, Islam T, Srivastava P, Othman Hadi HS. 2020. Precision of raw and bias-adjusted satellite precipitation estimations (TRMM, IMERG, CMORPH, and PERSIANN) over extreme flood events: Case study in Langat River basin, Malaysia. Journal of Water and Climate Change 11(S1): 322-342. https://doi.org/10.2166/wcc.2020.180

Srivastava A, Yetemen O, Saco PM, Rodríguez JF, Kumari N, Chun KP. 2022. Influence of orographic precipitation on coevolving landforms and vegetation in semi-arid ecosystems. Earth Surface Processes and Landforms 47: 2846-2862. https://doi.org/10.1002/esp.5427

Toté C, Patricio D, Boogaard H, van der Wijngaart R, Tarnavsky E, Funk C. 2015. Evaluation of satellite rainfall estimates for drought and flood monitoring in Mozambique. Remote Sensing 7: 1758-1776. https://doi.org/10.3390/rs70201758

Velásquez P, Messmer M, Raible CC. 2019. A new bias-correction method for precipitation over complex terrain suitable for different climate states: a case study using WRF (version 3.8.1). Geoscientific Model Development Discussions 13: 5007-5027. https://doi.org/10.5194/gmd-13-5007-2020

Villate García E, Morales Hernández JC, Romo Aguilar ML, García Concepción FO, Castillo Aja R. 2023. Potential of the CHIRPS database for extreme precipitation risk studies. Assessment in the State of Jalisco (Mexico). International Journal of Sustainable Development and Planning 18: 847-855. https://doi.org/10.18280/ijsdp.180320

Yeh NC, Chuang YC, Peng HS, Hsu KL. 2020. Bias adjustment of satellite precipitation estimation using ground-based observation: Mei-Yu front case studies in Taiwan. Asia-Pacific Journal of Atmospheric Sciences 56: 485-492. https://doi.org/10.1007/s13143-019-00152-7

Yu C, Hu D, Liu M, Wang S, Di Y. 2020. Spatio-temporal accuracy evaluation of three high-resolution satellite precipitation products in China area. Atmospheric Research 241: 104952. https://doi.org/10.1016/j.atmosres.2020.104952

Zhang Z, Koren V, Smith M, Reed S, Wang D. 2004. Use of next generation weather radar data and basin disaggregation to improve continuous hydrograph simulations. Journal of Hydrologic Engineering 9: 103-115. https://doi.org/10.1061/(ASCE)1084-0699(2004)9:2(103)

Statistical metrics for PT correction methodology at a sub-basin scale.

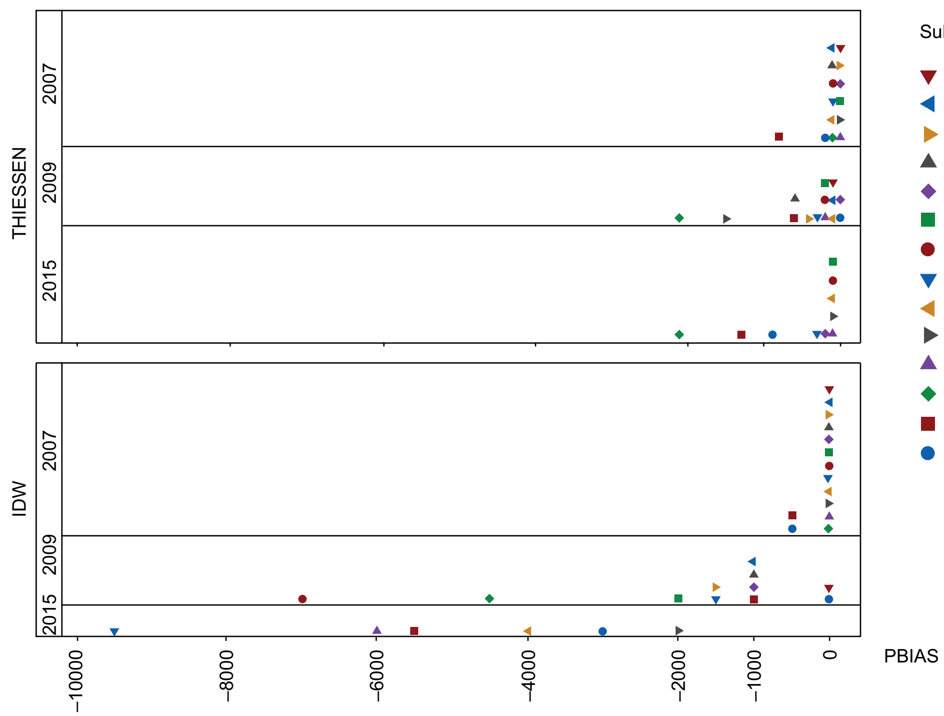

Fig. S1. Dots plots of percentual bias (PBIAS) for power transformation (PT) corrected satellite precipitation (SP) estimates vs. in-situ observations of maximum events in average (2007), dry (2009), and wet (2015) years.

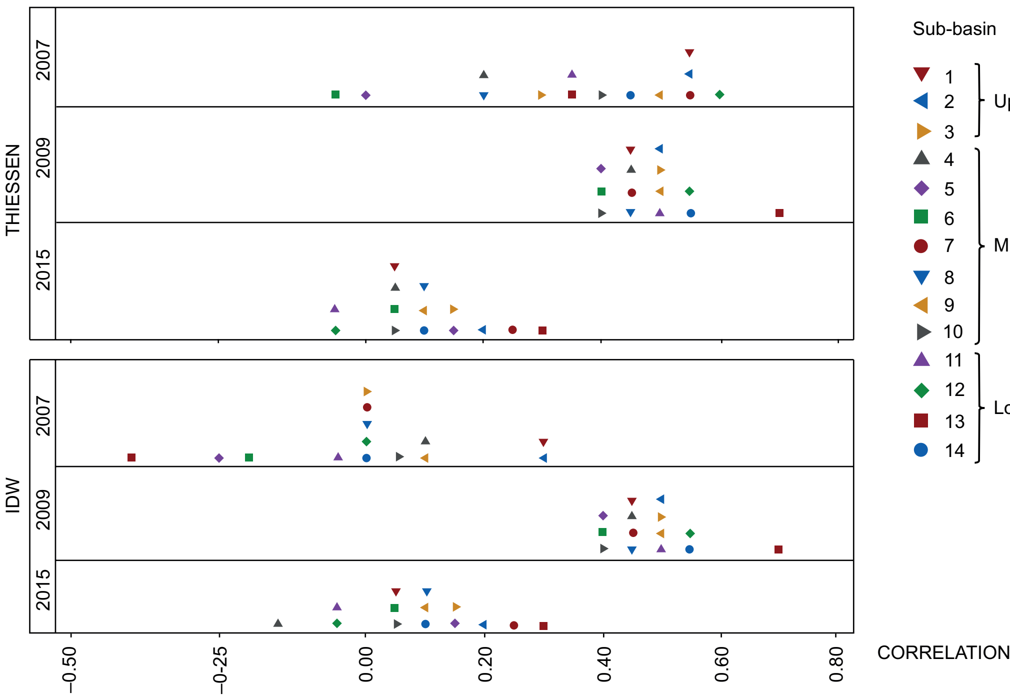

Fig. S2. Dots plots of correlation for power transformation (PT) corrected satellite precipitation (SP) estimates vs. in-situ observations of maximum events in average (2007), dry (2009), and wet (2015) years.

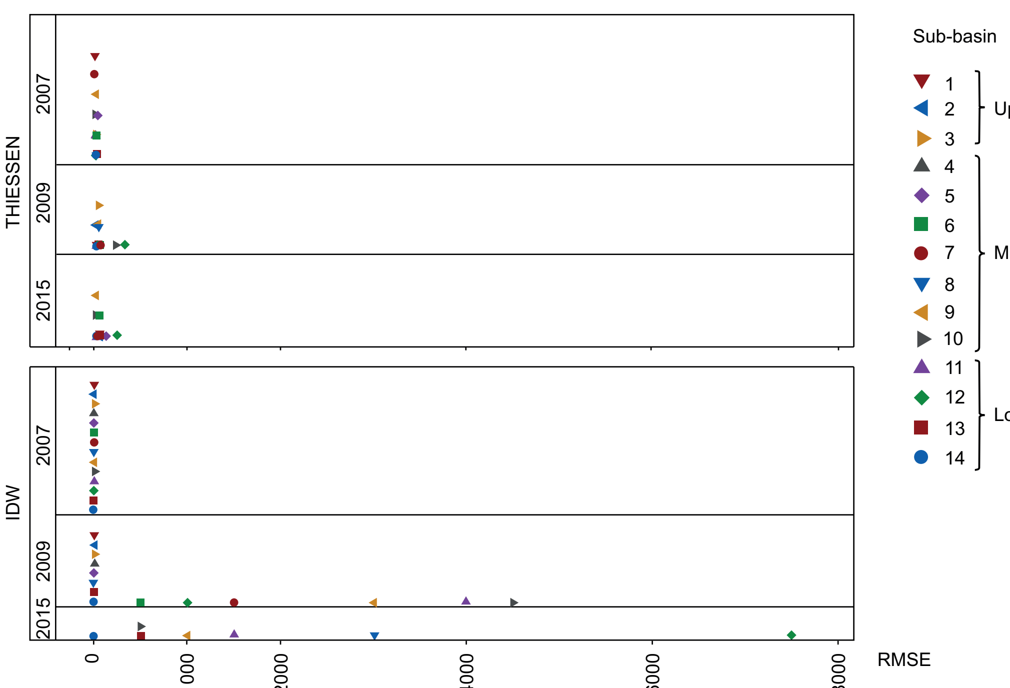

Fig. S3. Dots plots of root mean square error (RMSE) for power transformation (PT) corrected satellite precipitation (SP) estimates vs. in-situ observations of maximum events in average (2007), dry (2009), and wet (2015) years.

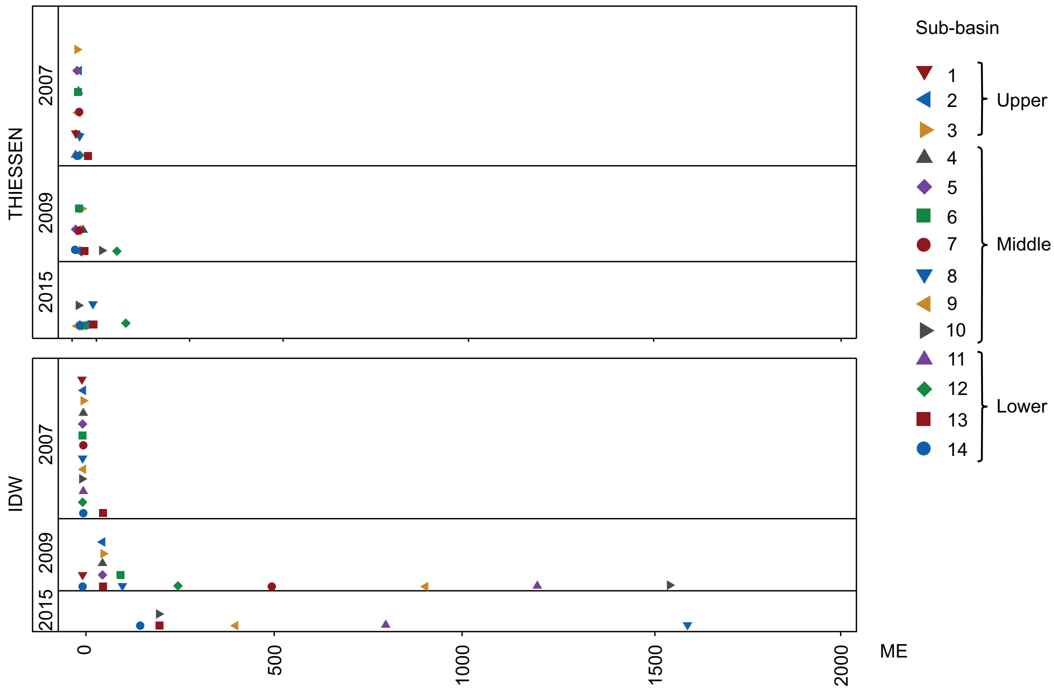

Fig. S4. Dots plots of mean error (ME) for power transformation (PT) corrected satellite precipitation (SP) estimates vs. in-situ observations of maximum events in average (2007), dry (2009), and wet (2015) years.

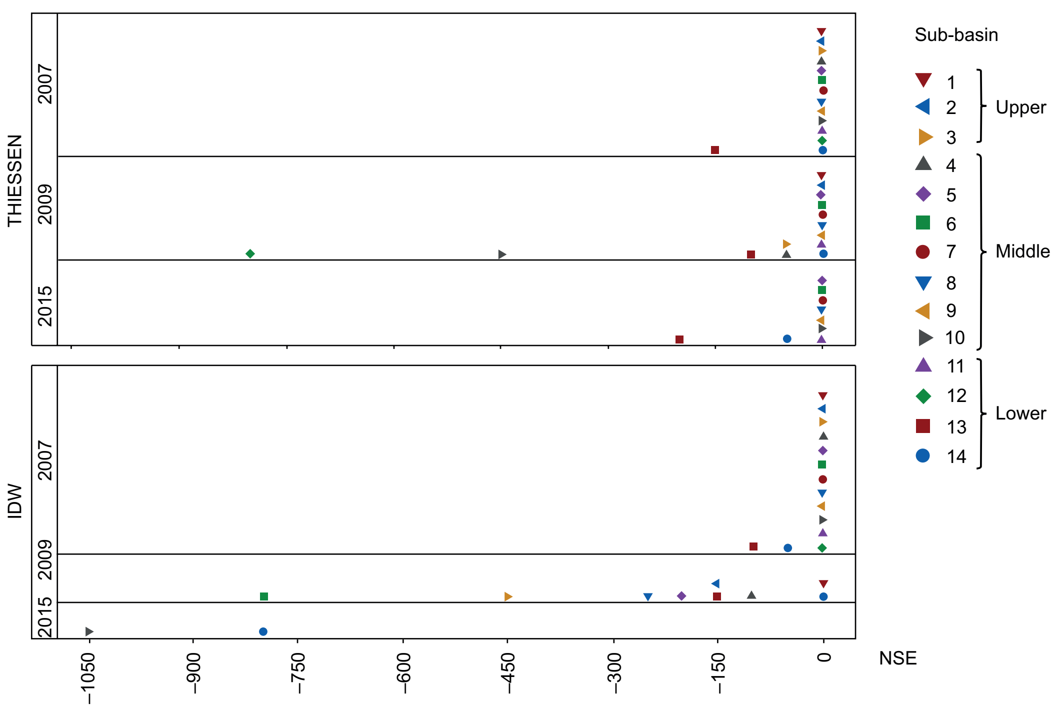

Fig. S5. Dots plots of Nash-Sutcliffe efficiency coefficient (NSE) for power transformation (PT) corrected satellite precipitation (SP) estimates vs. in-situ observations of maximum events in average (2007), dry (2009), and wet (2015) years.